



## ORIGINAL ARTICLE

# Bioenergy sorghum maintains photosynthetic capacity in elevated ozone concentrations

Shuai Li<sup>1,2,3</sup>  | Christopher A. Moller<sup>2,4</sup> | Noah G. Mitchell<sup>2,4</sup> | DoKyoung Lee<sup>1</sup> | Elizabeth A. Ainsworth<sup>1,2,4</sup> 

<sup>1</sup>Center for Advanced Bioenergy and Bioproducts Innovation, University of Illinois at Urbana-Champaign, Urbana, Illinois

<sup>2</sup>Carl R. Woese Institute for Genomic Biology, University of Illinois at Urbana-Champaign, Urbana, Illinois

<sup>3</sup>Institute for Sustainability, Energy, and Environment, University of Illinois at Urbana-Champaign, Urbana, Illinois

<sup>4</sup>Global Change and Photosynthesis Research Unit, USDA ARS, Urbana, Illinois

## Correspondence

Elizabeth A. Ainsworth, Global Change and Photosynthesis Research Unit, USDA ARS, 1201 W. Gregory Drive, 147 ERML, Urbana, IL 61801, USA.

Email: lisa.ainsworth@ars.usda.gov

## Funding information

U.S. Department of Energy, Grant/Award Number: DE-SC0018420

## Abstract

Elevated tropospheric ozone concentration ( $O_3$ ) significantly reduces photosynthesis and productivity in several  $C_4$  crops including maize, switchgrass and sugarcane. However, it is unknown how  $O_3$  affects plant growth, development and productivity in sorghum (*Sorghum bicolor* L.), an emerging  $C_4$  bioenergy crop. Here, we investigated the effects of elevated  $O_3$  on photosynthesis, biomass and nutrient composition of a number of sorghum genotypes over two seasons in the field using free-air concentration enrichment (FACE), and in growth chambers. We also tested if elevated  $O_3$  altered the relationship between stomatal conductance and environmental conditions using two common stomatal conductance models. Sorghum genotypes showed significant variability in plant functional traits, including photosynthetic capacity, leaf N content and specific leaf area, but responded similarly to  $O_3$ . At the FACE experiment, elevated  $O_3$  did not alter net  $CO_2$  assimilation ( $A$ ), stomatal conductance ( $g_s$ ), stomatal sensitivity to the environment, chlorophyll fluorescence and plant biomass, but led to reductions in the maximum carboxylation capacity of phosphoenolpyruvate and increased stomatal limitation to  $A$  in both years. These findings suggest that bioenergy sorghum is tolerant to  $O_3$  and could be used to enhance biomass productivity in  $O_3$  polluted regions.

## KEYWORDS

biomass, BWB model, chlorophyll fluorescence, MED model, photosynthesis, stomatal conductance

## 1 | INTRODUCTION

Rapid population growth is predicted to increase global demand for both food and energy (Tilman et al., 2009). Renewable biofuels (largely ethanol) derived from bioenergy feedstocks have the potential to replace fossil energy and reduce greenhouse gas emissions, and contribute to economic growth and energy security over the long-term (Reid, Ali, & Field, 2020; Tilman et al., 2009; Yuan, Tiller, Al-Ahman,

Stewart, & Stewart, 2008). Approximately 40% of the corn crop was used to produce ethanol in the United States over past 10 years (<https://afdc.energy.gov/data/10339>). However, ethanol can also be derived from other highly efficient  $C_4$  crops, such as sorghum, switchgrass and miscanthus (Calviño & Messing, 2012; Regassa & Wortmann, 2014; Rooney, Blumenthal, Bean, & Mullet, 2007; Schmer, Vogel, Mitchell, & Perrin, 2008; Wullschleger, Davis, Borsuk, Gunderson, & Lynd, 2010; Yuan et al., 2008). Sorghum (*Sorghum*

This is an open access article under the terms of the Creative Commons Attribution-NonCommercial-NoDerivs License, which permits use and distribution in any medium, provided the original work is properly cited, the use is non-commercial and no modifications or adaptations are made.

© 2020 The Authors. *Plant, Cell & Environment* published by John Wiley & Sons Ltd.

*bicolor* L.), a widely adapted and highly productive C<sub>4</sub> grass, has been identified as a promising feedstock for conversion to biofuels with a low input cost (Calviño & Messing, 2012; Regassa & Wortmann, 2014; Rooney et al., 2007). Sorghum requires minimal water and nutrient supply for its growth and can be cultivated on marginal croplands where water deficits, salinity and other constraints exist (Regassa & Wortmann, 2014). In contrast to maize, which stores about 85% starch in grains, many sorghum genotypes produce high biomass and accumulate a large amount of sugar in the stem that can be directly used for biofuel production (Calviño & Messing, 2012; Regassa & Wortmann, 2014; Rooney et al., 2007). Although sorghum is well-adapted to marginal environments and produces high biomass, the stability of production under atmospheric pollution, in particular O<sub>3</sub> pollution, is unknown.

Tropospheric ozone (O<sub>3</sub>) is a major secondary air pollutant formed from photochemical reactions of carbon monoxide (CO), methane and volatile organic compounds (VOCs) in the presence of nitrogen oxides (NO<sub>x</sub>) (Atkinson, 2000; Monks et al., 2015). Global O<sub>3</sub> concentrations have significantly increased since the Industrial Revolution due to increased O<sub>3</sub> precursor emissions (Monks et al., 2015; Young et al., 2013). Although O<sub>3</sub> concentrations have decreased in the eastern United States and parts of Europe over the past 20 years due to reductions of anthropogenic emissions, they are predicted to increase rapidly in developing regions such as south and east Asia and urban areas where O<sub>3</sub> concentration peaks of up to 120 nL L<sup>-1</sup> are measured (Chang, Petropavlovskikh, Cooper, Schultz, & Wang, 2017; Gao et al., 2015; Verma, Lakhani, & Kumari, 2017). Tropospheric O<sub>3</sub> is well recognized to have a deleterious impact on plant growth and development, resulting in a substantial loss of crop productivity and yield, as well as plant species diversity worldwide (Ainsworth, Yendrek, Sitch, Collins, & Emberson, 2012; Morgan, Mies, Bollero, Nelson, & Long, 2006; Wilkinson, Mills, Illidge, & Davies, 2012; Wittig, Ainsworth, Naidu, Karnosky, & Long, 2009). For example, it is estimated that up to 10% of maize yields are lost to O<sub>3</sub> pollution in the United States (McGrath et al., 2015). In addition, O<sub>3</sub> reduces global wheat yield by 85 Tg (million tonnes) and total crop yield (maize, soybean, rice and wheat combined) by 227 Tg annually (Mills et al., 2018a, 2018b). Therefore, there is strong evidence that decreased crop yield from O<sub>3</sub> pollution portends a significant threat to global food and energy security.

As a powerful oxidant, O<sub>3</sub> damages plants by entering the leaves through stomata. Once inside the leaf, O<sub>3</sub> can instantly react with plasmalemma lipids to produce other reactive oxygen species (ROS), including superoxide, hydrogen peroxide and hydroxyl radical, which directly damage cells and eventually lead to programmed cell death or accelerated senescence (Ainsworth, 2017; Fiscus, Booker, & Burkey, 2005; Li, Harley, & Niinemets, 2017; Long & Naidu, 2002). In general, O<sub>3</sub> exposure leads to reductions in the activity of ribulose-1,5-bisphosphate carboxylase/oxygenase (Rubisco) in the chloroplast, thereby reducing net CO<sub>2</sub> assimilation rate (A) and quantum yield of primary photochemistry, and increasing mitochondrial respiration which is associated with leaf senescence acceleration and yield loss (Ainsworth, 2017; Ainsworth et al., 2012; Fiscus et al., 2005; Flowers,

Fiscus, Burkey, Booker, & Dubois, 2007; Li et al., 2017, 2018; Morgan, Bernacchi, Ort, & Long, 2004; Yendrek, Erice, et al., 2017). Exposure to O<sub>3</sub> also results in decreased F<sub>v</sub>/F<sub>m</sub>, which represents the maximum quantum yield of PSII in dark-adapted leaves, and actual photochemical efficiency of PSII (Fiscus et al., 2005; Flowers et al., 2007; Guidi, Degl'Innocenti, Martinelli, & Piras, 2009; Li et al., 2017, 2018). Previous studies have also observed that exposure to elevated O<sub>3</sub> concentrations can alter leaf traits such as leaf mass per area (LMA) and leaf nitrogen (N) content, both of which strongly correlate to photosynthetic rate (Oikawa & Ainsworth, 2016; Oksanen, Riikonen, Kaakinen, Holopainen, & Vapaavuori, 2005). Despite the widely documented O<sub>3</sub> effects in many species, there is less information about genotypic variation in responses to O<sub>3</sub> in only a few species (Burkey, Booker, Ainsworth, & Nelson, 2012; Choquette, Ainsworth, Bezodis, & Cavanagh, 2020; Choquette et al., 2019; Frei, Tanaka, & Wissuwa, 2008; Yendrek, Eric, et al., 2017; Zhang et al., 2017). Identifying genotypic differences in O<sub>3</sub> tolerance is an important first step for breeding tolerant varieties that could be planted in high O<sub>3</sub> concentrations.

Chronic O<sub>3</sub> exposure may also cause incomplete stomatal closure, leading to greater water loss relative to net CO<sub>2</sub> assimilation (lower water-use efficiency) and decoupling of stomatal conductance (g<sub>s</sub>) and photosynthesis (Lombardozzi, Sparks, Bonan, & Levis, 2012; Paoletti & Grulke, 2010). Thus, understanding how O<sub>3</sub> affects photosynthetic carbon gain and water-use efficiency are crucial for improving O<sub>3</sub> tolerance in crops (Ainsworth, 2017; Ainsworth, Rogers, & Leakey, 2008; Leakey et al., 2019). The Ball-Woodrow-Berry (BWB) model and Medlyn (MED) models mathematically describe the leaf-level empirical relationship between photosynthesis, g<sub>s</sub> and environmental factors, and are widely used to predict carbon and water flux in both C<sub>3</sub> and C<sub>4</sub> plants under various field conditions such as different water availability and elevated CO<sub>2</sub> (Ball, Woodrow, & Berry, 1987; Franks et al., 2018; Leakey, Bernacchi, Ort, & Long, 2006; Medlyn et al., 2011; Miner & Bauerle, 2017; Wolz, Wertin, Abordo, Wang, & Leakey, 2017). The BWB and MED models are also used to describe variation in stomatal behaviour across species or plant functional types (Franks et al., 2018; Lin et al., 2015; Wolz et al., 2017). More recently, the BWB model has been applied to estimate the effect of elevated O<sub>3</sub> on the relationship between photosynthesis and g<sub>s</sub>. For example, elevated O<sub>3</sub> changed the relationship between photosynthesis and g<sub>s</sub> by increasing the intercept of the BWB model in rice (Masutomi et al., 2019), but did not alter BWB model parameters in switchgrass (Li, Courbet, Ourry, & Ainsworth, 2019). However, it is unclear how elevated O<sub>3</sub> concentration alters the parameters of these stomatal models in different sorghum lines.

Although much of our attention has been directed towards the negative responses of plant growth, development and productivity to O<sub>3</sub> in C<sub>3</sub> plants, the overall effects of O<sub>3</sub> on C<sub>4</sub> species remain less explored. Most C<sub>4</sub> species have Kranz-type leaf anatomy and accumulate Rubisco in the bundle sheath cells resulting in high water-use efficiency and high productivity. In addition, C<sub>4</sub> crops, such as corn and sorghum, may have a lower steady-state or modelled maximal stomatal conductance, implying less O<sub>3</sub> uptake than C<sub>3</sub> crops such as sunflower or rice (Hoshika, Osada, de Marco, Peñuelas, & Paoletti, 2018;

Lin et al., 2015; Zhen & Bugbee, 2020). Thus, C<sub>3</sub> and C<sub>4</sub> species might respond to O<sub>3</sub> differently. A few studies of O<sub>3</sub> response in maize (*Zea mays*) (Choquette et al., 2019, 2020; Leitao, Bethenod, & Biolley, 2007; Leitao, Maoret, & Biolley, 2007; Singh, Agrawal, Shahi, & Agrawal, 2014; Yendrek, Erice, et al., 2017; Yendrek, Tomaz, et al., 2017), switchgrass (*Panicum virgatum*) (Li et al., 2019) and sugarcane (*Saccharum* spp.) (Grant & Vu, 2009; Grant, Vu, Tew, & Veremis, 2012; Moura, Hoshika, Ribeiro, & Paoletti, 2018) have shown that elevated O<sub>3</sub> negatively impacts photosynthetic performance and biomass in C<sub>4</sub> species. With four species and numerous genotypes of maize and sugarcane examined, these studies have also shown that photosynthetic and yield responses to O<sub>3</sub> can vary among species and genotypes (Choquette et al., 2019, 2020; Li et al., 2019; Yendrek, Erice, et al., 2017).

Here we investigated the impacts of season-long elevated O<sub>3</sub> exposure on leaf photosynthetic traits and capacity, respiration, chlorophyll fluorescence, leaf functional traits, biomass and nutrient composition in several sorghum lines. Studies were conducted under fully open-air field conditions using free-air concentration enrichment (FACE) technology, which allows for long-term, continuous exposure to elevated O<sub>3</sub> and monitoring of plant traits under natural conditions with little or no perturbation of other environmental factors (Ainsworth & Long, 2005; Long, Ainsworth, Rogers, & Ort, 2004). In 2018, we studied 10 genotypes of sorghum grown at ambient and elevated O<sub>3</sub>, and in 2019, we investigated five of those genotypes a second time. We further examined photosynthetic response to elevated O<sub>3</sub> in four genotypes which were used in both 2018 and 2019 in a growth chamber experiment that minimized variation in other environmental parameters. The genotypes were chosen from a panel of 229 diverse biomass sorghum lines with significant variation in agronomic and physiological traits (Ferguson et al., 2020; Valluru et al., 2019). Given that sorghum may show a similar O<sub>3</sub> sensitivity as maize due to their close phylogenetic relationship (Lawrence & Walbot, 2007), we tested the hypotheses that elevated O<sub>3</sub> would: (a) reduce photosynthetic traits and capacity, such as net CO<sub>2</sub> assimilation, stomatal conductance, the maximum carboxylation capacity of phosphoenolpyruvate and CO<sub>2</sub> saturated photosynthetic capacity; (b) alter the relationship between stomatal conductance and photosynthesis as predicted by the BWB and MED model; and (c) decrease biomass and nutrient composition in sorghum lines. To our knowledge, this is the first study to examine how elevated O<sub>3</sub> affects photosynthesis and biomass in bioenergy sorghum genotypes, and provides important information for exploring O<sub>3</sub> sensitivity among C<sub>4</sub> species and identifying O<sub>3</sub> resistant bioenergy feedstocks.

## 2 | MATERIALS AND METHODS

### 2.1 | Field site, plant materials and growth condition

Sorghum (*S. bicolor* L.) lines were studied at the FACE facility (40°02'N, 88°14'W; [www.igb.illinois.edu/soyface/](http://www.igb.illinois.edu/soyface/)) in Champaign, IL in 2018 and 2019. The soil type at the FACE site is a Drummer, which

is typical in central Illinois (Ainsworth, Rogers, Nelson, & Long, 2004). Fertilizer (N, 200 kg ha<sup>-1</sup>) was applied before planting each year. Seeds of 10 sorghum genotypes (PI148093, PI329597, PI452577, PI452891, PI453336, PI457183A, PI665123, PI665129, TAM08001 and TAM17800) and five genotypes (PI329597, PI452891, PI457183A, PI665123 and TAM17800) were planted with a row spacing of 0.76 m and length of 3.96 m at a density of 5 plants m<sup>-2</sup> in four experimental blocks at the FACE facility on 10 May [DOY 130, also referred to as days after sowing (DAS) 0], 2018 and 31 May (DOY151/DAS 0), 2019, respectively. Each block consisted of two 20 m diameter octagonal plots, with one at ambient O<sub>3</sub> concentration (30–50 nL L<sup>-1</sup>) and another fumigated to elevated O<sub>3</sub> concentration (~100 nL L<sup>-1</sup>). After sorghum seeds were planted, the infrastructure for O<sub>3</sub> enrichment was installed and elevated O<sub>3</sub> plots were fumigated starting on 25 May (DOY 145/DAS 15) in 2018 and on 10 June (DOY 161/DAS 10) in 2019 (Figure S1). Operation of O<sub>3</sub> fumigation to the elevated plots followed the previously published protocols by Choquette et al. (2019), Morgan et al. (2004), Yendrek, Eric, et al. (2017) and Yendrek, Tomaz, et al. (2017). O<sub>3</sub> was generated by an O<sub>3</sub> generator (CFS-32G; Ozonia), mixed with air and delivered to the elevated plots with FACE technology. A chemiluminescence O<sub>3</sub> sensor (Model 49i, Thermo Scientific, MA) was used to monitor O<sub>3</sub> concentrations. The target O<sub>3</sub> concentration set point at the centre of the elevated plots was 100 nL L<sup>-1</sup>, with 8 hrs (10:00–18:00) fumigation per day throughout the growing season except when leaves were wet and/or when wind speed was lower than 0.5 m s<sup>-1</sup> (Choquette et al., 2019; Yendrek, Erice, et al., 2017; Yendrek, Tomaz, et al., 2017). O<sub>3</sub> fumigation was stopped on 13 August (DOY 225/DAS 95), 2018 and on 15 September (DOY 258/DAS 107), 2019 (Figure S1). Other weather conditions (the daily maximum and minimum air temperature and daily total precipitation) were recorded with an on-site weather station at the FACE facility (Figure S1).

### 2.2 | Leaf photosynthetic characteristics measurement

In situ leaf midday gas exchange and chlorophyll fluorescence were measured at three time points in both 2018 and 2019. All measurements were conducted with fully expanded sun-exposed leaves between 11:00 and 14:00 on sunny days following the protocols described in detail by Leakey, Uribeblanca, et al. (2006), Li et al. (2019) and Yendrek, Erice, et al. (2017). Considering strong variations in physiology and structure across leaf surface in large leaves (Li et al., 2013), all of the following measurements were made in the middle part of leaves. The third or fourth fully expanded leaf was selected for the first time point measurement in both 2018 and 2019. We used the same leaf for each of the following measurements, but if that leaf had senesced, then a younger leaf was measured. In 2018, the ninth leaf was measured on 2 and 3 July (DOY 183 and 184, referred to as DOY 183/DAS 53; time point A), the 9th or 10th leaf was measured on 23 and 24 July (DOY 204 and 205, referred to as DOY 204/DAS 74; time point B), and the 10th or 11th leaf was measured on

13 August (DOY 225/DAS 95; time point C) with portable photosynthesis systems (LI-6400, LICOR Biosciences, Lincoln, NE) (Figure S1). In 2019, the 10th leaf was measured on 24 and 25 July (DOY 205 and 206, referred to as DOY 205/DAS 54; time point A), the 11th leaf was measured on 8 and 9 August (DOY 220 and 221, referred to as DOY 220/DAS 69; time point B), and the 12th leaf was measured on 23 and 24 August (DOY 235 and 236, referred to as DOY 235/DAS 84; time point C) with portable photosynthesis systems (LI-6800, LICOR Biosciences, Lincoln, NE) (Figure S1). In all cases, the conditions within the leaf chamber cuvette were set to match the environmental ambient conditions (Table S1 for details). The measurements of the net CO<sub>2</sub> assimilation rates (*A*), stomatal conductance to water vapour (*g<sub>s</sub>*), the ratio of leaf intercellular CO<sub>2</sub> concentration to atmospheric CO<sub>2</sub> concentration (*c<sub>i</sub>:c<sub>a</sub>*) and chlorophyll fluorescence [midday PSII maximum efficiency (*F<sub>v</sub>'/F<sub>m</sub>'*), quantum yield of PSII ( $\Phi_{\text{PSII}}$ ), electron transport rate (ETR) and coefficient of photochemical quenching (*qP*)] under illumination were performed after stabilization of net photosynthesis for 3 ~ 5 min. The instantaneous water-use efficiency (*iWUE*) was calculated as the ratio of *A* to *g<sub>s</sub>*. In all cases, measurements were taken on two to four different individuals of each genotype within each plot.

Following in situ midday gas exchange measurements, the response of *A* to *c<sub>i</sub>* was measured on 3–6 July 2018 and on 9–22 August 2019. Two leaves from different individuals of each genotype within each plot which were used for time point A (2018) and time point B (2019) leaf gas exchange measurement were selected to measure *A/c<sub>i</sub>* response curves. Early in the morning, leaves from each experimental block were labelled and excised, immediately recut under water and quickly transported to the laboratory with the cut ends placed in water. Prior to *A/c<sub>i</sub>* curve measurement, leaves were then placed in 50 mL tubes filled with water and were exposed to saturating light levels under ambient CO<sub>2</sub> concentration for approximately 40 min to allow stomata to open and achieve a steady-state. After leaf enclosure, the initial conditions in the leaf cuvette were maintained at light intensity of 1800  $\mu\text{mol m}^{-2} \text{s}^{-1}$ , CO<sub>2</sub> concentration of 400  $\mu\text{mol mol}^{-1}$  and relative humidity of 65%. In 2018, the leaf chamber cuvette temperature was 26°C during the measurements and the CO<sub>2</sub> concentration was changed sequentially as follows: 400, 300, 200, 100, 50, 400, 600, 800, 1,000, 1,200  $\mu\text{mol mol}^{-1}$ . In 2019, the cuvette temperature was 28°C and CO<sub>2</sub> concentrations were: 400, 300, 200, 100, 50, 400, 600, 800, 1,000, 1,200 and 1,500  $\mu\text{mol mol}^{-1}$ . The maximum carboxylation capacity of phosphoenolpyruvate (*V<sub>pmax</sub>*) was calculated based on the initial slope of the *A/c<sub>i</sub>* curve (von Caemmerer, 2000), and CO<sub>2</sub> saturated photosynthetic capacity (*V<sub>max</sub>*) was estimated according to the horizontal asymptote of the *A/c<sub>i</sub>* curve by using a four-parameter non-rectangular hyperbolic function. Stomatal limitation to *A* (*S<sub>i</sub>*) was estimated for each genotype in ambient and elevated O<sub>3</sub> using mean values of *A/c<sub>i</sub>* curves in combination with in situ midday *c<sub>i</sub>* as previously described by Long and Bernacchi (2003), Markelz, Strellner, and Leakey (2011) and Yendrek, Eric, et al. (2017). Mean values of in situ midday *c<sub>i</sub>* for each genotype measured at time point A in 2018 and time point B in 2019 were used to calculate *S<sub>i</sub>*.

Following *A/c<sub>i</sub>* curve measurements, the leaf was removed from the chamber cuvette and dark-adapted for at least 50 min at room temperature. Afterwards, the leaf was enclosed in the leaf cuvette for 3 to 10 min, leaf dark respiration was measured under the following environmental conditions in the cuvette: leaf temperature was 28°C, light intensity was 0  $\mu\text{mol m}^{-2} \text{s}^{-1}$ , CO<sub>2</sub> concentration was 400  $\mu\text{mol mol}^{-1}$ , and relative humidity was 70% in 2018, and leaf temperature was 30°C, light intensity was 0  $\mu\text{mol m}^{-2} \text{s}^{-1}$ , CO<sub>2</sub> concentration was 420  $\mu\text{mol mol}^{-1}$  and relative humidity was 65% in 2019. To assess the impact of elevated O<sub>3</sub> on photosystem II (PS II) activity, the minimum (*F<sub>0</sub>*) and maximum (*F<sub>m</sub>*) dark-adapted fluorescence yield was measured by illuminating the leaf with a saturating irradiance of 7,000  $\mu\text{mol quanta m}^{-2} \text{s}^{-1}$ . The spatially averaged maximum dark-adapted quantum yield of photosystem II [*F<sub>v</sub>'/F<sub>m</sub>'* = (*F<sub>m</sub>* - *F<sub>0</sub>*) / *F<sub>m</sub>*] was calculated from *F<sub>0</sub>* and *F<sub>m</sub>*.

### 2.3 | Fitting BWB and MED models to leaf-level midday gas exchange data

The BWB model is defined as Ball et al. (1987):

$$g_s = m \frac{AH_s}{C_s} + g_0, \quad (1)$$

where *g<sub>s</sub>* is stomatal conductance to water vapour ( $\text{mol m}^{-2} \text{s}^{-1}$ ), *A* is net CO<sub>2</sub> assimilation rate ( $\mu\text{mol m}^{-2} \text{s}^{-1}$ ), *H<sub>s</sub>* is relative humidity (unitless) and *C<sub>s</sub>* is CO<sub>2</sub> concentration at the bottom of the leaf boundary layer ( $\mu\text{mol mol}^{-1}$ ) at the leaf surface. *m* is the slope which is directly related to the water-use efficiency and *g<sub>0</sub>* is the y-axis intercept which represents a minimum stomatal conductance.

The MED model (also known as stomatal optimization model) is defined by Medlyn et al. (2011):

$$g_s = 1.6 \left( 1 + \frac{g_M}{\sqrt{D}} \right) \frac{A}{C_s \sqrt{D}} + g_{0M}, \quad (2)$$

where *D* is the atmospheric vapour pressure deficit (kPa). *g<sub>M</sub>* is the model coefficient related to the slope and *g<sub>0M</sub>* is a minimum stomatal conductance similar to *m* and *g<sub>0</sub>*, respectively, in Equation (1). It should be noted that the term  $\frac{g_M}{\sqrt{D}}$  is large and dominates the term  $(1 + \frac{g_M}{\sqrt{D}})$ . Therefore, the linear relationship between *g<sub>s</sub>* and  $\frac{A}{C_s \sqrt{D}}$  was predicted.

The values of *A*, *g<sub>s</sub>*, *H<sub>s</sub>*, *C<sub>s</sub>* and *D* were obtained from LI-6400 in 2018 or LI-6800 in 2019 at three time point measurements of midday gas exchange. The slope (*m* and *g<sub>M</sub>*) and intercept (*g<sub>0</sub>* and *g<sub>0M</sub>*) were calculated based on the linear regression of BWB model and non-linear regression of MED model.

### 2.4 | Biomass, C and N content

All plants were harvested from 27–31 August 2018 and on 3 October 2019 (Figure S1). Three to five individuals of each genotype from each

plot were randomly selected to estimate plant biomass, C and N content. The number of leaves of each plant was counted and the total leaf area of each plant was measured by an area metre (LI-3100C, LICOR Biosciences, Lincoln, NE). Average leaf area was calculated as total leaf area/leaf number. Leaf and stem biomass were determined by weighing dry mass after drying at 70°C for 10 days. Plant biomass reported in this study is the sum of the leaf biomass and stem biomass. Leaf dry mass per area (LMA) was calculated as the ratio of leaf dry mass to total leaf area. Leaf and stem C and N concentrations were determined using a Costech 4010 elemental analyser (Costech Analytical Technologies, Inc., Valencia, CA). Leaf N content per unit area was calculated by multiplying mass-based N concentration by LMA.

## 2.5 | Growth chamber experiment

To further test the effects of elevated O<sub>3</sub> on photosynthetic traits of sorghum lines under controlled environmental conditions, a growth chamber experiment was performed. Four genotypes (PI329597, PI452891, PI457183A and PI665123) of sorghum were planted in 7.5 L plastic pots containing a commercial potting mix (Berger 6, Berger, Canada) on 4 February 2019. Three pots per each genotype were placed in eight growth chambers (Environmental Growth Chamber, Chagrin Falls, OH) under 60% relative humidity, 25/22°C day/night temperature and light intensity at plant level of 800 μmol m<sup>-2</sup> s<sup>-1</sup> from 08:00 to 20:00 hr. Four growth chambers were set as controls with ambient O<sub>3</sub> concentrations (30–50 nL L<sup>-1</sup>), while another four chambers were fumigated to an average elevated O<sub>3</sub> concentration of 150 nL L<sup>-1</sup> from 09:00 to 17:00 after sorghum seeds germinated. During the experiment, all plants were watered and fertilized as needed to maintain optimal growth conditions. O<sub>3</sub> was generated by an O<sub>3</sub> generator with UV light (HVAC 560 ozone generator, Crystal Air, Langley, Canada) and was monitored by a chemiluminescence O<sub>3</sub> sensor (Model 49i, Thermo Scientific, MA).

Gas exchange and chlorophyll fluorescence measurements were conducted on 5 March (DOY 64) and 12 March (DOY 71) after 4 and 5 weeks of fumigation on two to three fully expanded leaves (third or fourth leaf from the top) of different individuals of each genotype within each chamber using infrared gas analysers (LI-6800). The cuvette conditions were as follows: leaf temperature was 25°C, light intensity was 1,000 μmol m<sup>-2</sup> s<sup>-1</sup>, CO<sub>2</sub> concentration was 400 μmol mol<sup>-1</sup>, and relative humidity was 60%. A/c<sub>i</sub> response was measured on 6 March and 7 March using the same leaves and the microclimate of the cuvette was controlled with the following parameters: leaf temperature was 25°C, light intensity was 1,000 μmol m<sup>-2</sup> s<sup>-1</sup> and relative humidity was 60%. CO<sub>2</sub> concentration in the leaf cuvette was changed sequentially to 400, 300, 200, 100, 50, 400, 400, 600, 800, 1,000, 1,200 μmol mol<sup>-1</sup>. V<sub>pmax</sub> and V<sub>max</sub> were calculated, and S<sub>i</sub> was estimated using the mean values of c<sub>i</sub> measured on 5 March. Dark-adapted leaf respiration and F<sub>v</sub>/F<sub>m</sub> were also measured with leaf temperature at 25°C, light intensity at 0 μmol m<sup>-2</sup> s<sup>-1</sup>, CO<sub>2</sub> concentration at 400 μmol mol<sup>-1</sup>, and relative humidity at 60%, as described above. All plants were harvested on 18 March 2019. LMA, leaf and stem C and N concentrations were determined as described above.

## 2.6 | Statistical analysis

The main effects of O<sub>3</sub>, genotype and DOY and their interactions on gas exchange and chlorophyll fluorescence parameters were assessed by three-way ANOVA using multiplicative models followed by Tukey's post hoc test, separately for 2018, 2019 and for the growth chamber experiment using SPSS 16.0 (SPSS, Chicago, IL). The effects of O<sub>3</sub>, genotype and their interactions on A/c<sub>i</sub> curve parameters and growth parameters were assessed by two-way ANOVA, followed by Tukey's post hoc test. Linear regression was applied to the relationships between g<sub>s</sub> and c<sub>i</sub>:c<sub>a</sub>, between g<sub>s</sub> and  $\frac{A}{c_s}$ , between g<sub>s</sub> versus  $\frac{A}{c_s \sqrt{D}}$  and between leaf N content and LMA. The differences in slope and intercept of relationships (g<sub>s</sub> vs. c<sub>i</sub>:c<sub>a</sub>, g<sub>s</sub> vs.  $\frac{A}{c_s}$ , and leaf N vs. LMA) between ambient and elevated O<sub>3</sub> among sorghum lines were tested with ANCOVA. The values of MED model parameters were estimated from leaf-level gas exchange data fitted by non-linear regression using SigmaPlot (Systat Software Inc., Chicago, IL) and the differences in slope and intercept of MED model were tested with dummy variables. All statistical tests were considered significant at p < .05.

## 3 | RESULTS

### 3.1 | Leaf gas exchange and chlorophyll fluorescence response to elevated O<sub>3</sub>

Field measurements of in situ midday A and g<sub>s</sub> showed that both parameters decreased as leaves aged in 2018 and 2019 (Figures 1, 2 and 3). The genotypes differed significantly in A and g<sub>s</sub> in both years (Table 1). A and g<sub>s</sub> were not significantly different in elevated compared to ambient O<sub>3</sub> in most genotypes and at most time points (Figures 1, 2 and 3). c<sub>i</sub>:c<sub>a</sub> and iWUE were not consistently different in the sorghum genotypes or in ambient and elevated O<sub>3</sub> (Table 1). In addition, genotypic and time-dependent variation in chlorophyll fluorescence was observed for F<sub>v</sub>/F<sub>m</sub>, Φ<sub>PSII</sub>, ETR, and qP (Table 2). Growth in elevated O<sub>3</sub> did not have an effect on fluorescence parameters (Table 2).

In the growth chamber experiment, there was significant genotypic and time-dependent variation in the photosynthetic traits and chlorophyll fluorescence across four genotypes of sorghum (Table 3). Elevated O<sub>3</sub> significantly reduced g<sub>s</sub> in PI665123 but increased Φ<sub>PSII</sub>, ETR and qP in PI457183A on DOY 64 (p < .05; Figure S2). However, elevated O<sub>3</sub> did not alter photosynthetic traits and chlorophyll fluorescence across all genotypes (Table 3).

### 3.2 | Changes in A/c<sub>i</sub> curves, leaf respiration and dark-adapted chlorophyll fluorescence

Elevated O<sub>3</sub> led to a significant decrease in the maximum carboxylation capacity of phosphoenolpyruvate (V<sub>pmax</sub>) in both 2018 and 2019 (Table 4), with post hoc tests showing that V<sub>pmax</sub> was significantly lower in elevated O<sub>3</sub> in PI329597 and PI452891 in both years

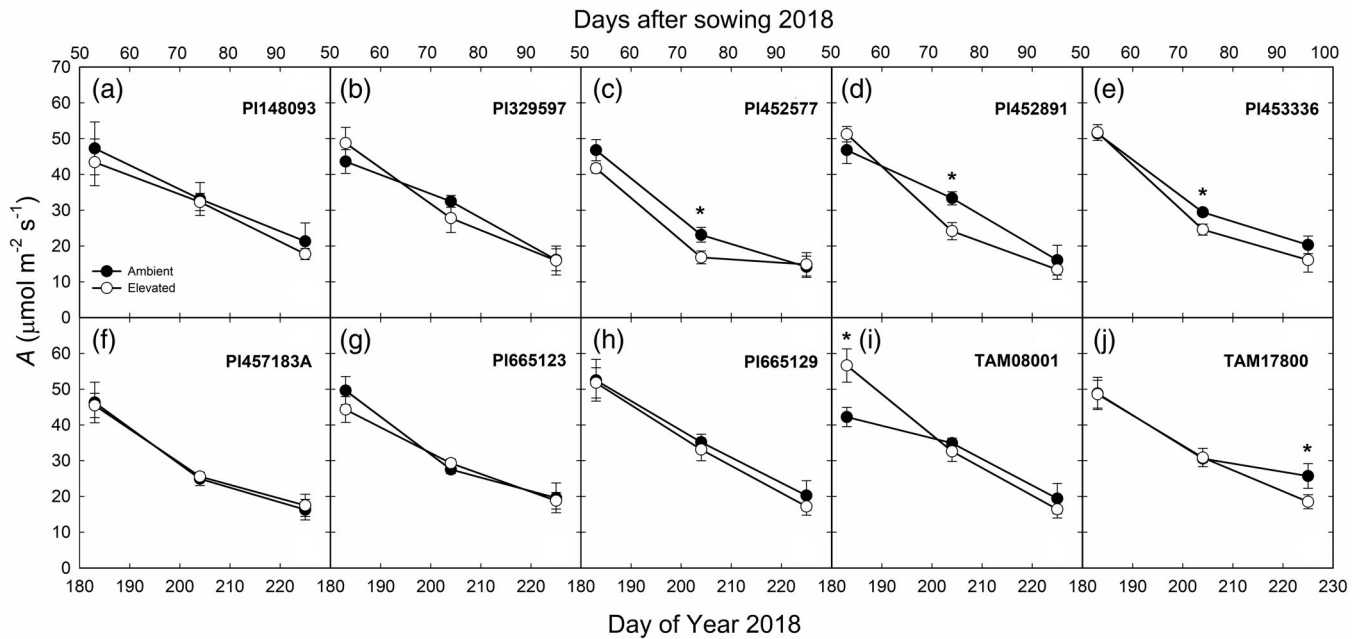


**FIGURE 1** In situ midday net  $\text{CO}_2$  assimilation rate ( $A$ ) measured in 10 genotypes of sorghum grown at ambient and elevated  $\text{O}_3$  on DOY 183, 204 and 225 in 2018. Error bars show SEs ( $n = 4$ ). Significant differences ( $p < .05$ ) between ambient and elevated  $\text{O}_3$  are indicated by asterisk

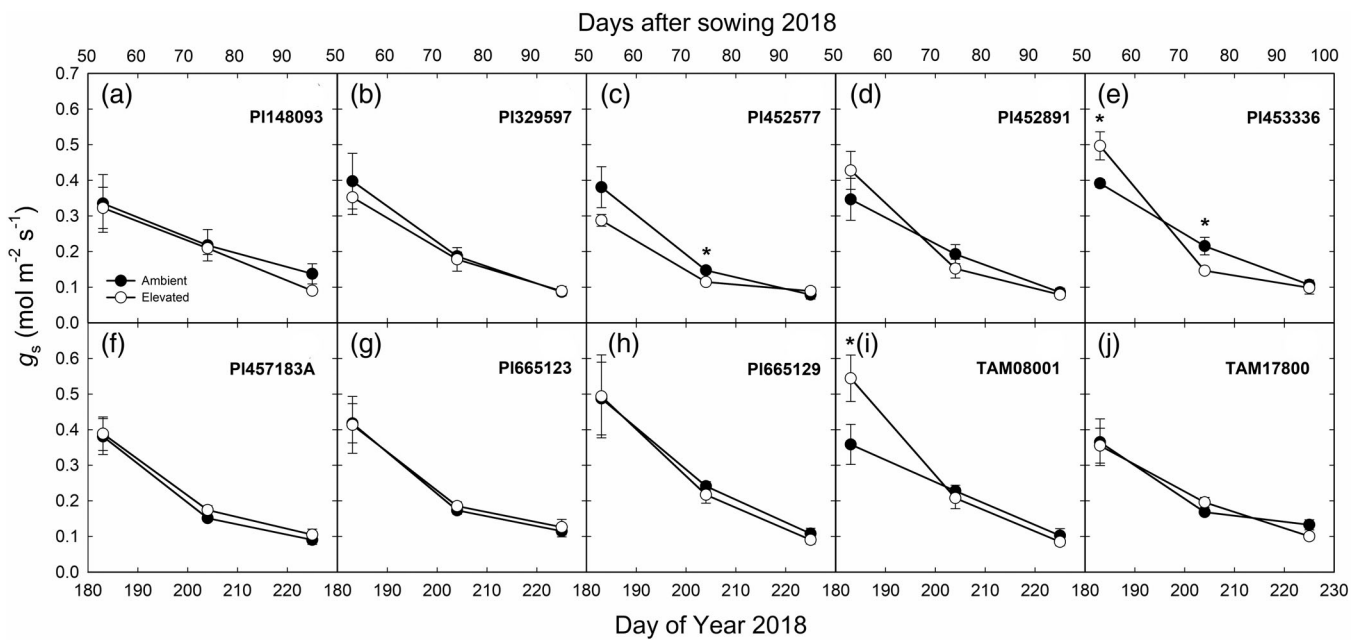


**FIGURE 2** In situ midday stomatal conductance ( $g_s$ ) measured in 10 genotypes of sorghum grown at ambient and elevated  $\text{O}_3$  on DOY 183, 204 and 225 in 2018. Error bars show SEs ( $n = 4$ ). Significant differences ( $p < .05$ ) between ambient and elevated  $\text{O}_3$  are indicated by asterisk

( $p < .05$ ; Figure 4a,b). However, there was no significant effect of  $\text{O}_3$  on the  $\text{CO}_2$  saturated photosynthetic capacity ( $V_{\max}$ ) in five genotypes of sorghum measured at FACE in 2018 and 2019 (Figure 4d,e and Table 4). There was no significant effect of elevated  $\text{O}_3$  on  $V_{\text{pmax}}$  or  $V_{\max}$  in any genotype in the growth chamber experiment, where photosynthetic capacity was significantly lower than those measured in the field (Figure 4c,f).

Stomatal limitation to  $A$  ( $S_i$ ) was also calculated from  $A/c_i$  curves in combination with in situ midday  $c_i$ . The mean  $c_i$  was below the inflexion point of the  $A/c_i$  curve in all genotypes in both years except for PI329597 in 2018 (Figure 5).  $S_i$  varied from 0.047 in PI329597 to 0.20 in TAM17800 in ambient  $\text{O}_3$  conditions in 2018, and from 0.063 in PI665123 to 0.22 in TAM17800 in elevated  $\text{O}_3$  (Figure 5a–e).  $S_i$  varied about 2.5-fold across genotypes in both ambient and elevated

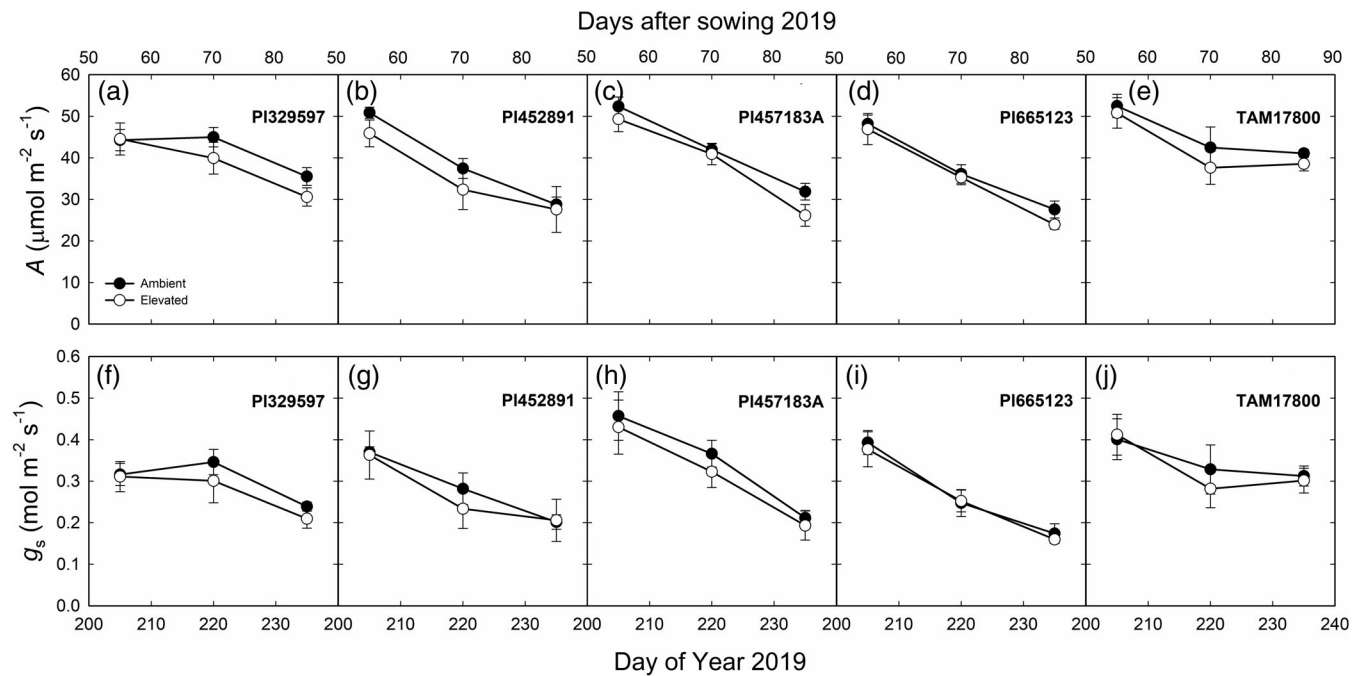


**FIGURE 3** In situ midday net CO<sub>2</sub> assimilation rate (*A*; a–e) and stomatal conductance (*g<sub>s</sub>*; f–j) measured in five genotypes of sorghum grown at ambient and elevated O<sub>3</sub> on DOY 205, 220 and 235 in 2019. Error bars show SEs (*n* = 4)

**TABLE 1** Analysis of variance (*F*, *p*) of midday net CO<sub>2</sub> assimilation rate (*A*), stomatal conductance (*g<sub>s</sub>*), the ratio of leaf intercellular CO<sub>2</sub> concentration to atmospheric CO<sub>2</sub> concentration (*c<sub>i</sub>:c<sub>a</sub>*), and instantaneous water-use efficiency (*iWUE*) measured in 10 genotypes of sorghum grown at ambient and elevated O<sub>3</sub> on DOY 183, 204 and 225 in 2018 and in 5 genotypes of sorghum grown at ambient and elevated O<sub>3</sub> on DOY 205, 220 and 235 in 2019 at the FACE facility.

	<i>A</i> (µmol m <sup>-2</sup> s <sup>-1</sup> )		<i>g<sub>s</sub></i> (mol m <sup>-2</sup> s <sup>-1</sup> )		<i>c<sub>i</sub>:c<sub>a</sub></i>		<i>iWUE</i> (µmol mol <sup>-1</sup> )	
	2018	2019	2018	2019	2018	2019	2018	2019
O <sub>3</sub>	2.62, 0.11	<b>7.93, 0.006</b>	0.001, 0.97	2.09, 0.15	3.83, 0.052	1.53, 0.22	3.38, 0.067	0.001, 0.98
Genotype (G)	<b>3.41, 0.001</b>	<b>5.99, &lt;0.001</b>	<b>2.31, 0.018</b>	<b>4.36, 0.003</b>	1.86, 0.06	<b>4.06, 0.005</b>	1.48, 0.16	<b>2.59, 0.042</b>
O <sub>3</sub> × G	0.53, 0.85	0.081, 0.99	0.55, 0.84	0.11, 0.98	0.64, 0.76	0.65, 0.63	0.75, 0.67	0.54, 0.71
Day of year (DOY)	<b>412.8, &lt;0.001</b>	<b>86.7, &lt;0.001</b>	<b>281.6, &lt;0.001</b>	<b>43.9, &lt;0.001</b>	<b>60.3, &lt;0.001</b>	1.41, 0.25	<b>109.1, &lt;0.001</b>	2.62, 0.079
O <sub>3</sub> × DOY	1.68, 0.19	0.18, 0.83	1.17, 0.31	0.29, 0.75	0.013, 0.99	1.76, 0.18	0.014, 0.99	1.49, 0.23
G × DOY	1.06, 0.40	<b>2.66, 0.011</b>	1.14, 0.32	<b>2.39, 0.022</b>	1.34, 0.17	<b>2.27, 0.029</b>	1.64, 0.054	<b>2.28, 0.029</b>
O <sub>3</sub> × G × DOY	0.93, 0.55	0.31, 0.96	0.91, 0.57	0.12, 0.99	1.36, 0.16	0.37, 0.94	1.64, 0.055	0.31, 0.96

Note: Significant effects are shown in boldface.

O<sub>3</sub> in 2019 (Figure 5f–j). For most genotypes, the range of *S<sub>i</sub>* estimated in ambient and elevated O<sub>3</sub> were completely overlapping, suggesting that there was not a biologically significant change in *S<sub>i</sub>* in elevated O<sub>3</sub>. In the growth chamber experiment, the mean *c<sub>i</sub>* was above the inflexion point of the *A/c<sub>i</sub>* curve in all genotypes under both ambient and elevated O<sub>3</sub> and again the range of estimated *S<sub>i</sub>* values was totally overlapping in ambient and elevated O<sub>3</sub> (Figure S3).

Leaf respiration and maximum dark-adapted quantum yield of photosystem II (*F<sub>v</sub>/F<sub>m</sub>*) were not significantly different between ambient and elevated O<sub>3</sub> or across 5 genotypes in 2018 and 2019 at the FACE experiment (Figure S4a,b,d,e and Table S4). A significant decrease in *F<sub>v</sub>/F<sub>m</sub>* in PI457183A was detected in the growth

chambers, resulting in a significant O<sub>3</sub> × genotype treatment interaction (Figure S4f and Table S2).

### 3.3 | Relationship between *g<sub>s</sub>* and *c<sub>i</sub>:c<sub>a</sub>*

*c<sub>i</sub>:c<sub>a</sub>* showed a highly significant positive correlation with *g<sub>s</sub>* across 10 genotypes and 3 measurement dates under both ambient and elevated O<sub>3</sub> in 2018 (*p* < .001; Figure 6a). The correlation was also significant when the data were subset to examine only the five genotypes that were measured in both 2018 and 2019 (*p* < .001; Figure 6b,c). In both years, elevated O<sub>3</sub> did not alter the slope of the relationship

**TABLE 2** Analysis of variance ( $F$ ,  $p$ ) of midday PSII maximum efficiency ( $F_v'/F_m'$ ), quantum yield of PSII ( $\Phi_{PSII}$ ), electron transport rate (ETR), and coefficient of photochemical quenching ( $qP$ ) measured in 10 genotypes of sorghum grown at ambient and elevated  $O_3$  on DOY 183, 204 and 225 in 2018 and in 5 genotypes of sorghum grown at ambient and elevated  $O_3$  on DOY 205, 220 and 235 in 2019 at the FACE facility.

	$F_v'/F_m'$		$\Phi_{PSII}$		ETR ( $\mu\text{mol m}^{-2} \text{s}^{-1}$ )		$qP$	
	2018	2019	2018	2019	2018	2019	2018	2019
$O_3$	2.91, 0.09	1.12, 0.29	2.51, 0.12	1.28, 0.26	2.59, 0.11	1.26, 0.26	1.47, 0.23	0.86, 0.36
Genotype (G)	<b>2.96, 0.003</b>	1.63, 0.17	<b>2.21, 0.024</b>	<b>6.12, 0.001</b>	<b>2.27, 0.02</b>	<b>7.74, &lt;0.001</b>	<b>2.47, 0.011</b>	<b>6.40, &lt;0.001</b>
$O_3 \times G$	1.35, 0.22	0.45, 0.78	0.32, 0.97	1.25, 0.30	0.33, 0.97	1.24, 0.30	0.44, 0.91	1.79, 0.14
Day of year (DOY)	0.85, 0.43	<b>35.5, &lt;0.001</b>	<b>340.9, &lt;0.001</b>	<b>41.2, &lt;0.001</b>	<b>355.7, &lt;0.001</b>	<b>68.4, &lt;0.001</b>	<b>343.5, &lt;0.001</b>	<b>20.5, &lt;0.001</b>
$O_3 \times \text{DOY}$	1.39, 0.25	0.27, 0.76	0.73, 0.48	0.67, 0.52	0.77, 0.47	0.82, 0.44	0.69, 0.50	1.01, 0.37
$G \times \text{DOY}$	0.63, 0.87	1.87, 0.074	1.17, 0.29	<b>2.16, 0.038</b>	1.21, 0.26	<b>2.97, 0.005</b>	1.37, 0.15	<b>2.13, 0.041</b>
$O_3 \times G \times \text{DOY}$	0.53, 0.94	0.23, 0.98	0.67, 0.84	0.32, 0.96	0.68, 0.83	0.29, 0.97	0.54, 0.94	0.30, 0.97

Note: Significant effects are shown in boldface.

**TABLE 3** Analysis of variance ( $F$ ,  $p$ ) of net  $\text{CO}_2$  assimilation rate ( $A$ ), stomatal conductance ( $g_s$ ), the ratio of leaf intercellular  $\text{CO}_2$  concentration to atmospheric  $\text{CO}_2$  concentration ( $c_i:c_a$ ), and instantaneous water-use efficiency ( $iWUE$ ), PSII maximum efficiency ( $F_v'/F_m'$ ), quantum yield of PSII ( $\Phi_{PSII}$ ), electron transport rate (ETR) and coefficient of photochemical quenching ( $qP$ ) measured in four genotypes of sorghum grown at ambient and elevated  $O_3$  on DOY 64 and 71 in 2019 in the growth chambers

	$A$	$g_s$	$c_i:c_a$	$iWUE$	$F_v'/F_m'$	$\Phi_{PSII}$	ETR	$qP$
	( $\mu\text{mol m}^{-2} \text{s}^{-1}$ )	( $\text{mol m}^{-2} \text{s}^{-1}$ )		( $\mu\text{mol mol}^{-1}$ )			( $\mu\text{mol m}^{-2} \text{s}^{-1}$ )	
$O_3$	0.014, 0.91	2.34, 0.13	5.09, 0.030	3.79, 0.059	0.36, 0.55	0.54, 0.47	0.54, 0.47	0.84, 0.36
Genotype (G)	<b>4.38, 0.010</b>	<b>5.78, 0.002</b>	<b>3.96, 0.015</b>	<b>4.82, 0.006</b>	<b>7.69, &lt;0.001</b>	<b>3.02, 0.042</b>	<b>3.02, 0.042</b>	<b>5.05, 0.005</b>
$O_3 \times G$	0.86, 0.47	0.93, 0.44	0.28, 0.84	0.10, 0.96	1.34, 0.28	0.91, 0.45	0.91, 0.45	1.20, 0.32
Day of year (DOY)	<b>37.5, &lt;0.001</b>	<b>32.3, &lt;0.001</b>	0.037, 0.85	0.11, 0.74	<b>13.9, 0.001</b>	<b>9.46, 0.004</b>	<b>9.46, 0.004</b>	<b>4.84, 0.034</b>
$O_3 \times \text{DOY}$	0.12, 0.74	0.77, 0.39	0.0040, 0.95	0.033, 0.86	0.26, 0.61	0.97, 0.33	0.97, 0.33	0.90, 0.35
$G \times \text{DOY}$	2.46, 0.077	1.66, 0.19	0.35, 0.79	0.32, 0.81	<b>7.04, 0.001</b>	<b>4.61, 0.008</b>	<b>4.61, 0.008</b>	2.70, 0.059
$O_3 \times G \times \text{DOY}$	0.33, 0.81	0.68, 0.57	0.78, 0.51	0.93, 0.44	0.55, 0.65	0.40, 0.75	0.40, 0.75	0.28, 0.84

Note: Significant effects are shown in boldface.

**TABLE 4** Analysis of variance ( $F$ ,  $p$ ) of the maximum carboxylation capacity of PEPC ( $V_{pmax}$ ) and  $\text{CO}_2$ -saturated photosynthetic rate ( $V_{max}$ ) measured in five genotypes of sorghum grown at ambient and elevated  $O_3$  at FACE in 2018 and 2019 and in four genotypes of sorghum grown at ambient and elevated  $O_3$  in growth chamber

		2018	2019	Chamber
		$V_{pmax}$	$O_3$	<b>6.58, 0.016</b>
	Genotype (G)	<b>3.09, 0.03</b>	<b>2.75, 0.047</b>	<b>21.8, &lt;0.001</b>
	$O_3 \times G$	1.25, 0.311	0.37, 0.83	0.55, 0.65
$V_{max}$	$O_3$	1.93, 0.18	2.13, 0.16	2.35, 0.14
	G	1.24, 0.32	<b>5.72, 0.002</b>	<b>17.5, &lt;0.001</b>
	$O_3 \times G$	0.17, 0.95	0.41, 0.80	0.82, 0.50

Note: Significant effects are shown in boldface.

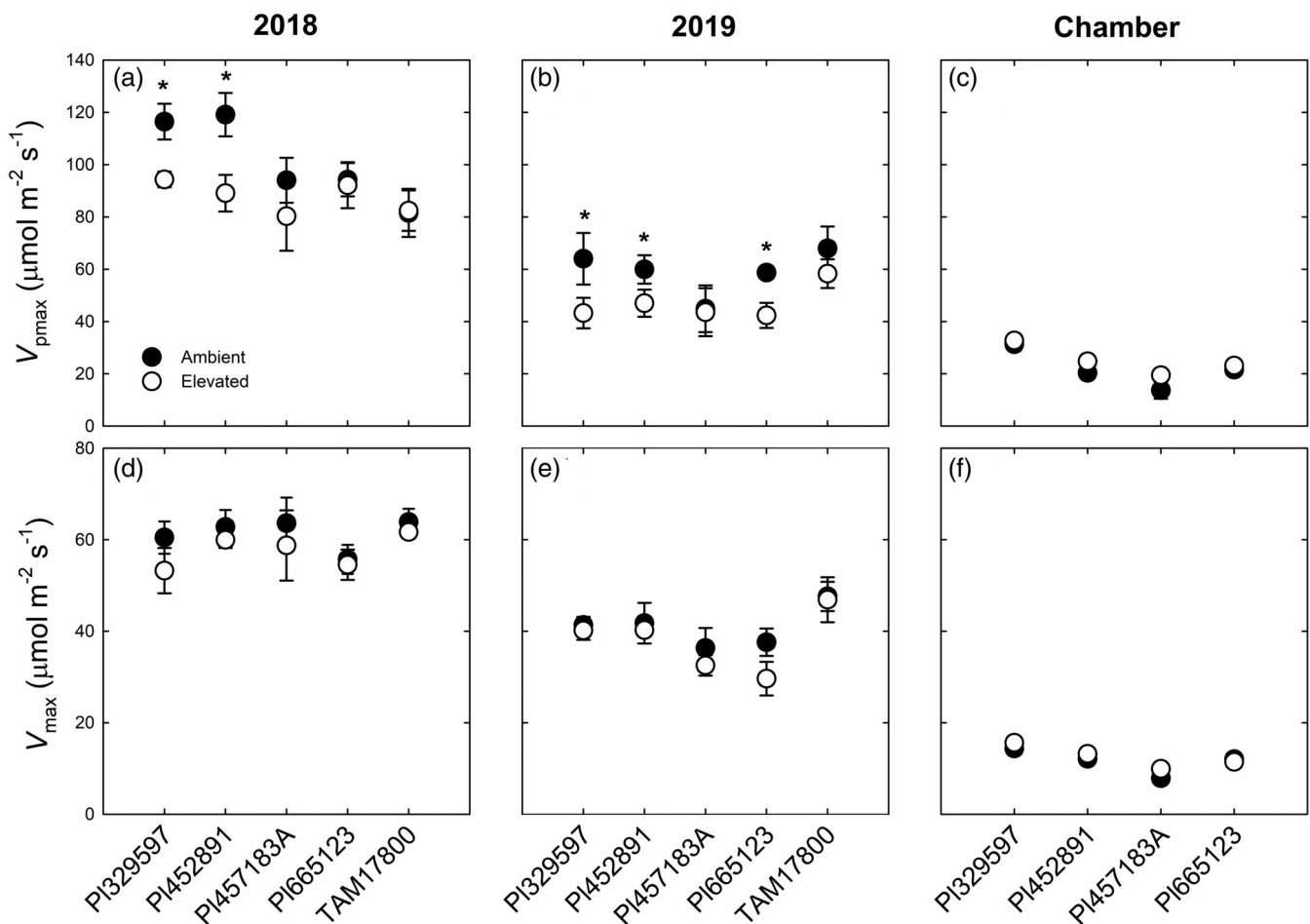
between  $g_s$  and  $c_i:c_a$  (Figure 6). A significant effect of  $O_3$  on the intercept was observed only in 2019 with all five genotypes ( $p < .05$ ; Figure 6c). The relationship between  $g_s$  and  $c_i:c_a$  was also tested at different time points to assess how prolonged exposure to  $O_3$  may have

impacted the correlation. The correlation between  $g_s$  and  $c_i:c_a$  weakened over time in both 2018 and 2019 (Figure S5). A significant decrease in intercept was detected only in time point C in 2019 ( $p < .05$ ; Figure S5i). Independent analysis of the genotypes also revealed variation in the correlation between  $g_s$  and  $c_i:c_a$ , but  $O_3$  did not alter the slopes or intercepts of the relationship in any individual genotype (Figure S6).

### 3.4 | Comparison of BWB and MED model parameters across genotypes

The BWB and MED models both empirically predict the relationship between  $g_s$  and  $A$  under varying environmental conditions.  $g_s$  was strongly correlated with  $\frac{A H_s}{C_s}$  and  $\frac{A}{C_s \sqrt{D}}$  across all genotypes or different measurement dates in both ambient and elevated  $O_3$  ( $p < .001$ ; Figures S7 and S8). Growth under elevated  $O_3$  did not alter the slope or intercept of the BWB and MED models across all genotypes in 2018 (Table 5), but a significant decrease in the intercept was observed in the BWB model in 2019 for five genotypes ( $p < .05$ ;





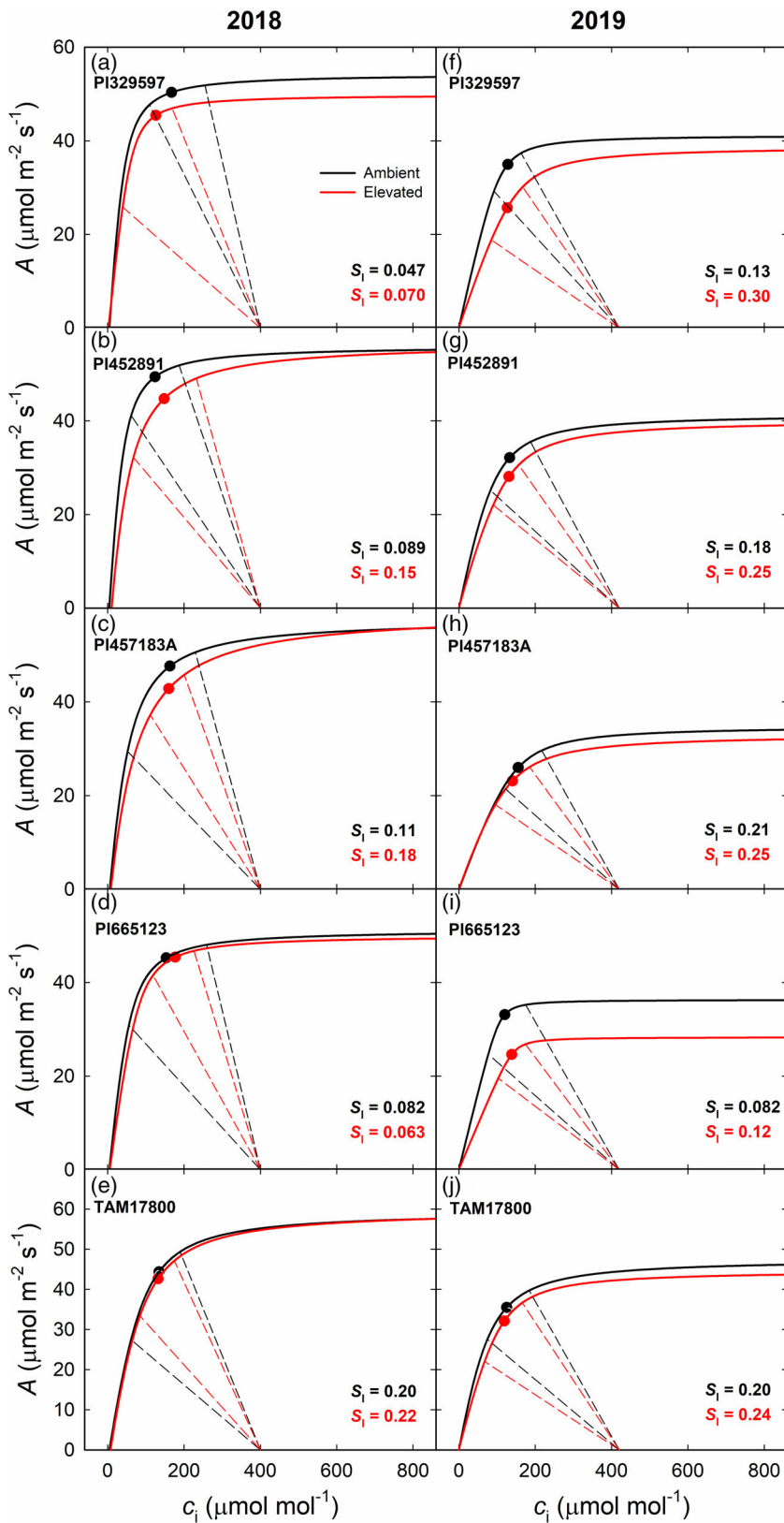
**FIGURE 4** Maximum carboxylation capacity of PEPC ( $V_{pmax}$ , a–c) and  $CO_2$ -saturated photosynthetic rate ( $V_{max}$ , d–f) measured in five genotypes of sorghum grown at ambient and elevated  $O_3$  in 2018 (a,d) and 2019 (b,e), and in four genotypes of sorghum grown at ambient and elevated  $O_3$  in growth chamber (c,f). Error bars show SEs ( $n = 4$ ). Significant differences ( $p < .05$ ) between ambient and elevated  $O_3$  are indicated by asterisk

Table 5). In the growth chamber, both the slope and intercept were significantly affected by the  $O_3$  treatment across four genotypes in BWB and MED models ( $p < .05$ ; Table 5). For the FACE experiments, there was no statistical difference in the slope or intercept of the BWB and MED models in ambient and elevated  $O_3$  measured in time point A in either year (Table S3). For both models, a reduction of the intercept of  $O_3$  exposed leaves was found in the measurement of 5 genotypes at time point B in 2018 ( $p < .05$ ; Table S3) and 10 or 5 genotypes at time point C, when leaves were older in 2018 ( $p < .05$ ; Table S3). Elevated  $O_3$  significantly decreased the intercept of BWB model, but increased the slope of MED model in the five genotypes measured in common at time point C in both 2018 and 2019 (Table S3).  $g_s$  also showed a highly significant correlation with  $\frac{A}{C_s}$  and  $\frac{A}{C_s \sqrt{D}}$  in each genotype measured in both years, but a significant effect of  $O_3$  on the slope of both models was only observed in PI329597 ( $p < .01$ ; Table S4) in 2018 and PI452891 ( $p < .05$ ; Table S4) in 2019. In addition,  $O_3$  reduced the slope of the MED model in PI452577 in 2018 ( $p < .05$ ; Table S4).  $O_3$  did not alter the intercept of either the BWB or MED model in any individual

genotype in 2018 or 2019 (Table S4). Both slope and intercept varied substantially among all genotypes in both models in 2018 and 2019. In 2018, the BWB model slope ranged across genotypes from  $4.04 \pm 0.43$  to  $5.46 \pm 0.60$  under ambient and from  $3.44 \pm 0.24$  to  $5.33 \pm 0.70$  under elevated  $O_3$ , and the MED model slope varied from  $1.25 \pm 0.23$  to  $2.25 \pm 0.26$  under ambient and from  $0.88 \pm 0.15$  to  $2.13 \pm 0.42$  under elevated  $O_3$  (Table S4). In 2019, the slope of BWB model varied among genotypes from  $3.23 \pm 0.33$  to  $4.85 \pm 0.64$  and from  $3.91 \pm 0.28$  to  $4.50 \pm 0.39$  under ambient and elevated  $O_3$ , respectively, and the MED model slope varied from  $1.44 \pm 0.27$  to  $3.37 \pm 0.61$  under ambient and from  $2.10 \pm 0.26$  to  $2.90 \pm 0.30$  under elevated  $O_3$  (Table S4).

### 3.5 | Elevated $O_3$ had no effect on plant biomass but changed nutrient composition

Leaf number, leaf size and leaf biomass, stem biomass and plant height varied greatly across different genotypes in 2018 and 2019 (Figures 7



**FIGURE 5** Summary of  $A/c_i$  response curves (solid lines) and  $\text{CO}_2$  supply functions (dashed lines) for five genotypes of sorghum grown at ambient  $\text{O}_3$  (black lines) and elevated  $\text{O}_3$  (red lines) in 2018 (a–e) and 2019 (f–j). The dashed lines represent the observed maximum and minimum midday  $c_i$ , and the points indicate the mean values ( $n = 4$ ) of midday  $c_i$  which was measured under  $\text{CO}_2$  concentration of  $400 \mu\text{mol mol}^{-1}$  at time point A in 2018 and  $420 \mu\text{mol mol}^{-1}$  at time point B in 2019. Stomatal limitation ( $S_i$ ) for each genotype under ambient and elevated  $\text{O}_3$  is reported in each panel. For all  $A/c_i$  regressions,  $r^2 > 0.98$  and  $p < .0001$

and S9). In 2018, elevated  $\text{O}_3$  significantly decreased the ratio of leaf biomass to stem biomass in PI452577 ( $p < .05$ ; Figure 7g) and average leaf area in PI148093 ( $p < .05$ ; Figure S9e), but increased leaf number and total leaf area in PI665123 ( $p < .05$  and  $p < .001$ ; Figure S9a,c). Across all genotypes in 2018, the effect of elevated  $\text{O}_3$  was only

observed in the ratio of leaf biomass to stem biomass (Figure 7g) and total leaf area (Figure S9c) and there was no significant elevated  $\text{O}_3 \times$  genotype interaction in any trait (Figures 7 and S9). These traits were not significantly different between ambient and elevated  $\text{O}_3$  across five genotypes in 2019 (Figures 7 and S9).

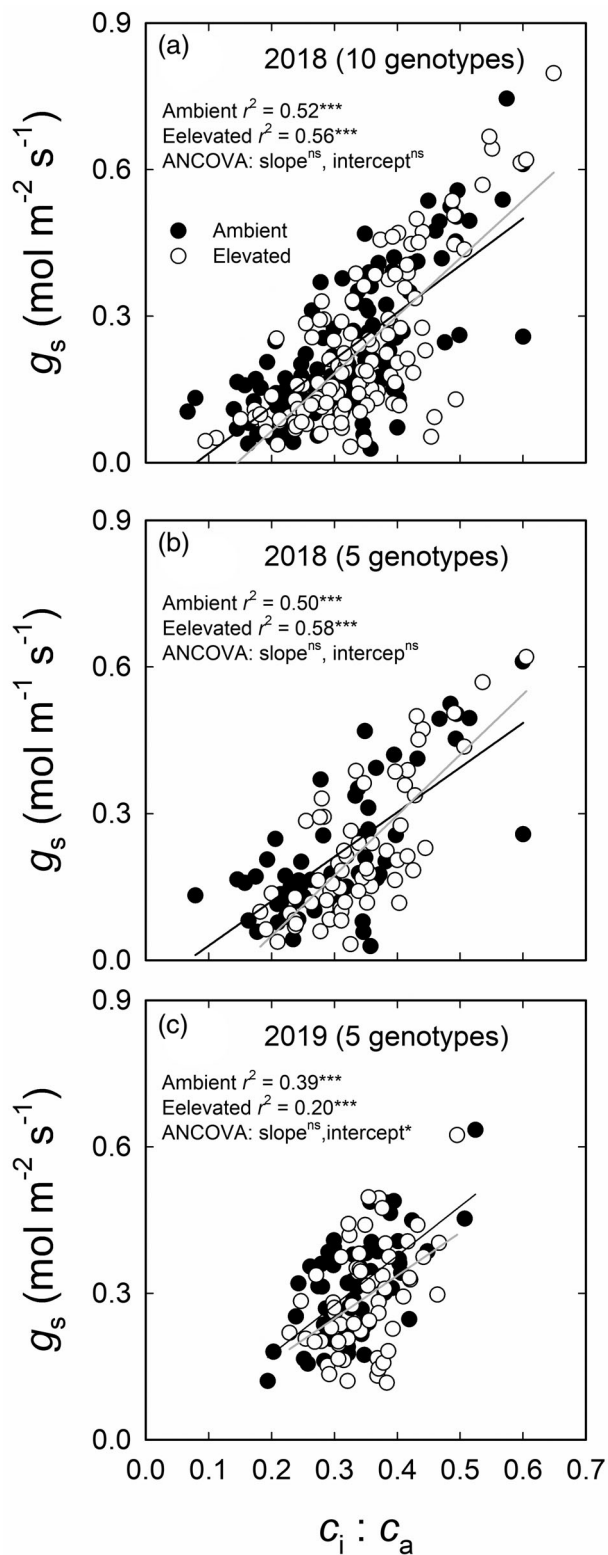


**FIGURE 6** The relationship between stomatal conductance ( $g_s$ ) and the ratio of leaf intercellular  $\text{CO}_2$  concentration to atmospheric  $\text{CO}_2$  concentration ( $C_i : C_a$ ) in 10 genotypes (a) and 5 genotypes (b) of sorghum grown under ambient and elevated  $\text{O}_3$  measured on DOY 183, 204 and 225 in 2018 and in 5 genotypes (c) of sorghum grown under ambient and elevated  $\text{O}_3$  measured on DOY 205, 220 and 235 in 2019. The data were fitted by linear regressions. ns, no significant difference ( $p > .05$ ); \* $p < .05$ ; \*\*\* $p < .001$

Genotypic variation in leaf mass per area (LMA), leaf and stem C and N was found in 2018, 2019 and the growth chamber experiment (Table 6). The elevated  $\text{O}_3$  impact on LMA, leaf and stem C and N in 2018 was not consistent with the lack of an effect on these traits in 2019 and in the growth chamber experiment (Table 6). In particular, leaf N tended to be greater in ambient compared to elevated  $\text{O}_3$  in 2018 (Figure 8a,b,d,e). The correlation between LMA and leaf N was examined on a mass ( $N_{\text{mass}}$ ) and an area ( $N_{\text{area}}$ ) basis. Both mass and area-based concentrations of leaf N were positively correlated with LMA (Figure 8). However, correlations between LMA and  $N_{\text{area}}$  were stronger than those between LMA and  $N_{\text{mass}}$  (Figure 8). Elevated  $\text{O}_3$  decreased the intercept of the relationship between LMA and  $N_{\text{area}}$  (Figure 8a) and between LMA and  $N_{\text{mass}}$  (Figure 8d,e) in 2018 but did not change either the slope or the intercept of the correlation in five genotypes in 2019 (Figure 8f). In addition, no significant correlations were observed between LMA and  $N_{\text{mass}}$  under ambient conditions and between LMA and  $N_{\text{area}}$  under ambient and elevated  $\text{O}_3$  in the growth chamber experiment (Figure S10).

## 4 | DISCUSSION

Sorghum (*S. bicolor* L.), a highly productive  $\text{C}_4$  grass used for biofuel production, has not been examined for response to elevated  $\text{O}_3$  in the field. In this study, we exposed different genotypes of biomass sorghum to elevated  $\text{O}_3$  over two growing seasons in the field using FACE technology, and in a growth chamber experiment to test sorghum response to  $\text{O}_3$  in the absence of other stresses common in field environments. We found evidence of considerable variation among sorghum genotypes in photosynthesis, plant biomass and nutrient concentrations. Across all genotypes, we also found that elevated  $\text{O}_3$  did not alter photosynthetic characteristics, the BWB and MED relationship or plant biomass, despite reduced  $V_{\text{pmax}}$  and decreased leaf nitrogen in 2018. However,  $\text{O}_3$  effects on nutrient composition were not consistent in both years at the FACE facility or with growth chamber measurements.

### 4.1 | Effects of elevated $\text{O}_3$ on photosynthetic characteristic

$\text{O}_3$  is well known to negatively impact plant growth, development and productivity (e.g. Ainsworth et al., 2012; Fiscus et al., 2005; Morgan et al., 2006; Wilkinson et al., 2012; Wittig et al., 2009). Prior FACE studies with maize and switchgrass found that  $\sim 100 \text{ nL L}^{-1}$   $\text{O}_3$  significantly reduced net photosynthetic carbon assimilation ( $A$ ) and stomatal conductance ( $g_s$ ) (Choquette et al., 2019, 2020; Li et al., 2019; Yendrek, Erice, et al., 2017). However, we found that elevated  $\text{O}_3$  ( $\sim 100 \text{ nL L}^{-1}$ ) did not alter either  $A$  or  $g_s$  in most genotypes across three time points, and two field growing seasons (Figures 1, 2 and 3). In addition, there was no evidence of any effect of elevated  $\text{O}_3$  on midday chlorophyll fluorescence across all genotypes (Table 2), which is not consistent with prior observation with switchgrass at FACE (Li et al., 2019). Therefore, these results indicate that sorghum might

**TABLE 5** BWB and MED model slope coefficients and minimum stomatal conductance derived from leaf-level midday gas exchange measurements in 2018 and 2019 at the FACE and in 2019 in the growth chambers

		2018 (10 genotypes)		2018 (5 genotypes)	2019	Chamber
BWB	Slope ( $\pm SE$ )	Amb	4.64 (0.14)	4.57 (0.20)	3.99 (0.22)	<b>2.86 (0.38)</b>
		Ele	4.57 (0.12)	4.34 (0.15)	4.22 (0.14)	<b>2.03 (0.28)</b>
	Intercept ( $\pm SE$ )	Amb	-0.016 (0.0084)	-0.017 (0.012)	<b>-0.037 (0.020)</b>	<b>0.0036 (0.011)</b>
		Ele	-0.0057 (0.0075)	0.0034 (0.0084)	<b>-0.041 (0.011)</b>	<b>0.013 (0.0086)</b>
MED	Slope ( $\pm SE$ )	Amb	1.62 (0.085)	1.57 (0.12)	2.18 (0.19)	<b>1.16 (0.30)</b>
		Ele	1.65 (0.076)	1.52 (0.087)	2.35 (0.16)	<b>0.50 (0.38)</b>
	Intercept ( $\pm SE$ )	Amb	-0.052 (0.0091)	-0.052 (0.013)	-0.12 (0.025)	<b>-0.00060 (0.012)</b>
		Ele	-0.045 (0.0082)	-0.036 (0.0091)	-0.12 (0.019)	<b>0.011 (0.0090)</b>

Note: Significant differences ( $p < .05$ ) between ambient and elevated  $O_3$  are shown in boldface. Abbreviations: BWB, Ball-Woodrow-Berry; MED, Medlyn.

have a greater  $O_3$  tolerance than other  $C_4$  species. However, historical maize yield loss due to  $O_3$  was greater in dry years with high temperatures (McGrath et al., 2015). This suggests that  $O_3$  sensitivity in maize is highly dependent on environmental conditions such as water availability and growing season temperature. Further work is needed to understand how  $O_3$  sensitivity varies across genotypes and  $C_4$  species in side-by-side experiments.

Long-term exposure has been positively correlated with leaf damage and loss of stomatal control or stomatal sluggishness in ageing leaves (Paoletti & Grulke, 2010). However, both  $c_i:c_a$  and  $iWUE$  remained constant (Table 1) suggesting that there was no uncoupling of  $A$  and  $g_s$  and stomatal limitations to  $A$  ( $S_i$ ) were minimized (Figure 5). It has been suggested that reductions in photosynthesis to  $O_3$  in soybean and maize were determined by biochemical limitation, not stomatal limitation (Choquette et al., 2020; Morgan et al., 2004; Yendrek, Eric, et al., 2017). In this study, elevated  $O_3$  led to increased  $S_i$  in both years (Figure 5). However, the range of estimated  $S_i$  values in ambient and elevated  $O_3$  completely overlapped, suggesting that changes in  $S_i$  in elevated  $O_3$  were not biologically significant. There was a surprising result that  $V_{pmax}$  was reduced by elevated  $O_3$  in PI329597, PI452891 and PI665123 (Figure 4), yet this change in capacity did not result in lower photosynthetic performance. This could be because changes in  $V_{pmax}$  were not sufficient to limit gas exchange. Furthermore, quantum yield of primary photochemistry in dark-adapted leaves ( $F_v/F_m$ ) did not change in response to elevated  $O_3$  in all genotypes (Figure S4 and Table S2), suggesting that photosystem II photochemistry was not damaged by a season-long  $O_3$  exposure. In fact, no visible foliar injury was observed due to  $O_3$  on all genotypes in either year. Consistent with FACE studies, the growth chamber measurements provide further evidence that sorghum was tolerant to elevated  $O_3$ , with no changes in photosynthetic capacity measured.

The correlation between  $CO_2$  fixation and  $g_s$  and empirical relationship between  $A$  and  $g_s$  are crucial in understanding how elevated  $O_3$  impairs photosynthetic capacity (Choquette et al., 2019; Li et al., 2019; Masutomi et al., 2019).  $c_i:c_a$  was positively correlated with  $g_s$  in ambient and elevated  $O_3$  (Figure 6). Growth at elevated  $O_3$  reduced the intercept of relationship between  $c_i:c_a$  and  $g_s$  across all genotypes in 2019

(Figure 6c). However, elevated  $O_3$  did not alter the slope or intercept of the relationship within each genotype in 2018 and 2019 (Figure S6). This further suggests that the genotypes have a similar  $O_3$  response.

The BWB and MED models provide information about the leaf-level empirical relationship between  $A$  and  $g_s$  with environmental factors (Ball et al., 1987; Medlyn et al., 2011). Previous studies reported that the BWB relationship was altered by elevated  $O_3$  in  $O_3$ -sensitive rice cultivars (Masutomi et al., 2019), but it was not affected in switchgrass (Li et al., 2019). Although the MED model has been increasingly used to determine terrestrial stomatal behaviour at a global scale because of its application of optimization principles (Franks et al., 2018; Lin et al., 2015), whether elevated  $O_3$  alters the MED parameters has not been tested. In this study, we investigated the slope parameter in both the BWB and MED models, and found that elevated  $O_3$  did not alter the slope of either model in any sorghum genotype across the growing season (Tables 5 and S3). This is consistent with no changes in  $iWUE$  at elevated  $O_3$  in 2018 and 2019 (Table 1). In addition, there was a similar  $O_3$ -induced reduction in the slope of both models as leaves aged in 2018 (Table S3). Furthermore, the changes in intercept by  $O_3$  were very similar when using either the BWB or MED model across all genotypes or all time point measurements (Tables 5, S3 and S4). Although the slope and intercept of both models varied substantially among all genotypes under ambient and elevated  $O_3$  in both 2018 and 2019, such similarities of BWB and MED suggest that both models would have a similar performance when fitted to leaf-level midday gas exchange data and that all genotypes respond to  $O_3$  similarly. This is consistent with recent side-by-side comparisons in the predictive strength of the BWB and MED models for other species and environmental conditions (Franks et al., 2018; Wolz et al., 2017).

## 4.2 | Impact of elevated $O_3$ on plant biomass and nutrient composition

A successful bioenergy crop requires biomass yield stability under a changing climate. How elevated  $O_3$  alters plant biomass in  $C_4$  crops is

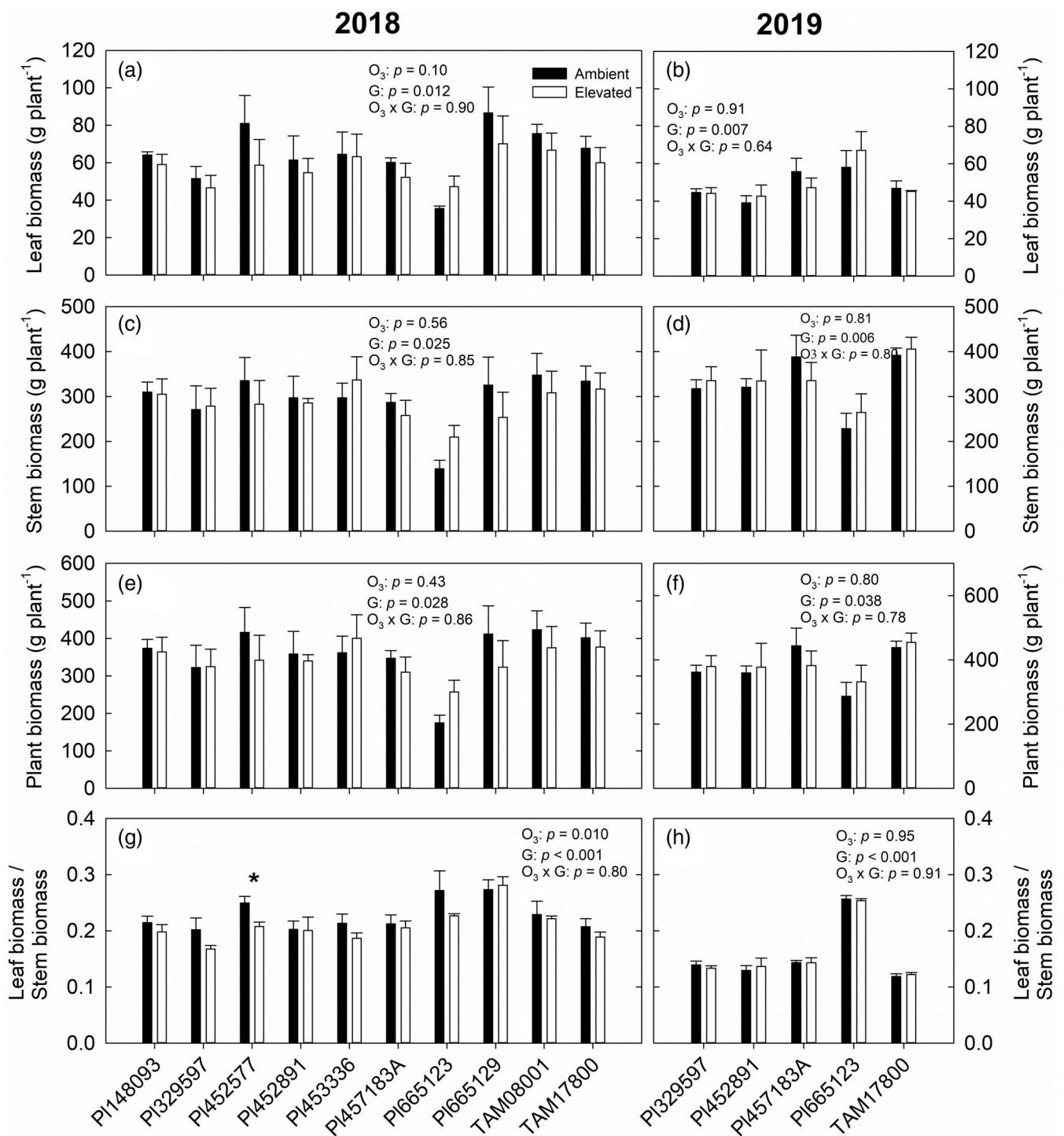


**FIGURE 7** Leaf biomass (a,b), stem biomass (c,d), plant biomass (e,f) and the ratio of leaf biomass to stem biomass (g,h) measured in sorghum genotypes grown at ambient and elevated O<sub>3</sub> in 2018 (a,c,e,g) and 2019 (b,d,f,h). Error bars show SEs ( $n = 4$ ). Significant differences ( $p < .05$ ) between ambient and elevated O<sub>3</sub> are indicated by asterisk

currently unclear. Previous studies have shown that O<sub>3</sub> significantly reduced plant biomass in growth chamber maize and greenhouse sugarcane (Grantz & Vu, 2009; Leitao, Bethenod, & Biolley, 2007). In our study, we observed no changes in plant biomass to O<sub>3</sub> across all sorghum genotypes in both years in the field (Figure 7), consistent with a past study of switchgrass using FACE technology (Li et al., 2019). This

further suggests that sorghum is tolerant to O<sub>3</sub> and biomass yield stability will not be influenced by O<sub>3</sub> pollution. Since enclosure experiments may amplify downregulation of plant production in response to O<sub>3</sub> due to differences in growth conditions including limited soil volume in pots and greater exposure of leaves O<sub>3</sub> based on air flow within chambers (Ainsworth & Long, 2005; Long et al., 2004), further

**TABLE 6** Analysis of variance (*F*, *p*) of LMA, leaf and stem nitrogen and carbon content measured in 10 genotypes of sorghum grown at ambient and elevated O<sub>3</sub> in 2018 and in 5 genotypes of sorghum grown at ambient and elevated O<sub>3</sub> in 2019

Year	Genotype	LMA (g m <sup>-2</sup> )	Leaf N (g m <sup>-2</sup> )	Leaf N (%)	Leaf C (%)	Leaf C: N	Stem N (%)	Stem C (%)	Stem C: N	Leaf N/Stem N	Leaf C/Stem C
2018	O <sub>3</sub>	<b>7.38, 0.009</b>	1.66, 0.203	<b>39.62, &lt;0.001</b>	<b>4.46, 0.039</b>	<b>44.68, &lt;0.001</b>	<b>12.34, 0.001</b>	<b>4.83, 0.032</b>	<b>13.60, &lt;0.001</b>	<b>4.40, 0.040</b>	0.005, 0.94
	Genotype (G)	<b>4.62, &lt;0.001</b>	<b>10.24, &lt;0.001</b>	<b>10.822, &lt;0.001</b>	<b>24.66, &lt;0.001</b>	<b>7.62, &lt;0.001</b>	<b>7.92, &lt;0.001</b>	<b>5.02, &lt;0.001</b>	<b>5.90, &lt;0.001</b>	<b>8.33, &lt;0.001</b>	<b>12.5, &lt;0.001</b>
	O <sub>3</sub> × G	0.61, 0.78	0.81, 0.61	0.91, 0.52	0.46, 0.89	0.795, 0.62	0.78, 0.63	1.29, 0.26	0.81, 0.61	0.44, 0.91	0.82, 0.60
	O <sub>3</sub>	3.12, 0.084	<b>6.09, 0.020</b>	2.76, 0.11	1.20, 0.28	2.98, 0.094	2.33, 0.14	0.001, 0.98	3.27, 0.081	1.48, 0.23	0.71, 0.40
2019	G	<b>17.9, &lt;0.001</b>	<b>28.9, &lt;0.001</b>	<b>3.34, 0.021</b>	<b>134.1, &lt;0.001</b>	<b>3.73, 0.014</b>	<b>38.9, &lt;0.001</b>	<b>13.2, &lt;0.001</b>	<b>38.3, &lt;0.001</b>	<b>42.0, &lt;0.001</b>	<b>47.9, &lt;0.001</b>
	O <sub>3</sub> × G	0.47, 0.76	1.02, 0.41	1.74, 0.17	0.13, 0.97	1.68, 0.18	0.38, 0.82	0.22, 0.93	0.88, 0.49	1.58, 0.21	0.13, 0.97
	O <sub>3</sub>	<b>4.70, 0.043</b>	<b>5.61, 0.029</b>	1.06, 0.32	2.42, 0.14	1.14, 0.30	1.25, 0.28	3.14, 0.092	1.91, 0.18	0.15, 0.70	<b>7.47, 0.013</b>
	G	<b>15.8, &lt;0.001</b>	0.89, 0.46	2.07, 0.14	<b>4.73, 0.013</b>	2.22, 0.12	<b>7.57, 0.002</b>	<b>18.6, &lt;0.001</b>	<b>13.1, &lt;0.001</b>	<b>9.44, &lt;0.001</b>	<b>25.7, &lt;0.001</b>
Chamber	O <sub>3</sub> × G	<b>4.65, 0.013</b>	1.59, 0.22	0.99, 0.42	<b>6.82, 0.003</b>	0.50, 0.69	0.31, 0.82	2.82, 0.067	0.94, 0.44	0.77, 0.53	<b>10.1, &lt;0.001</b>

Note: Significant effects are shown in boldface.  
Abbreviation: LMA, leaf mass per area.

studies are needed to gain an insight into the effect of elevated O<sub>3</sub> on plant biomass in more C<sub>4</sub> species in the field.

Nitrogen (N) is a primary component of the nucleotides and proteins that are essential for photosynthetic apparatus and reactions (Evans, 1989). Elevated O<sub>3</sub> typically reduces leaf N in many species, with the negative effects being counteracted by additional N treatment (Oikawa & Ainsworth, 2016; Yendrek, Leisner, & Ainsworth, 2013). In this study, reductions in both leaf and stem N to O<sub>3</sub> in 2018 were observed (Table 6). Interestingly, the decline in N did not cause any changes in photosynthetic performance and plant biomass (Figure 7). In addition, no differences in leaf and stem N were found in ambient and elevated O<sub>3</sub> across five genotypes in 2019 which is consistent with a previous study on switchgrass (Li et al., 2019). Given the different O<sub>3</sub> effects on leaf and stem N in both years, it could be because LMA was only altered by O<sub>3</sub> in 2018 (Table 6). In addition, sorghum genotypes under elevated O<sub>3</sub> showed lower leaf N at a given LMA in 2018, implying higher photosynthetic N use efficiency compared to plants under ambient O<sub>3</sub> (Figure 8).

Taken together, we found strong evidence of O<sub>3</sub> tolerance in a range of sorghum biomass genotypes. In addition, our results suggest that sorghum might have a greater O<sub>3</sub> tolerance than other C<sub>4</sub> species. But what mechanisms underlie the great O<sub>3</sub> tolerance in sorghum biomass genotypes? Morgan et al. (2004) suggested that O<sub>3</sub> concentration varied with leaf position in the canopy because upper canopy leaves may have higher stomatal conductance and O<sub>3</sub> uptake than lower canopy leaves. Biomass sorghum continuously added vegetative tissue throughout the growing season in central Illinois because of its photoperiod sensitivity (Maughan et al., 2012; Rooney & Aydin, 1999), in contrast to maize, which stops vegetative growth ~9 to 10 weeks after emergence (Bollero, Bullock, & Hollinger, 1996). Continuous development of vegetative tissue may be one of the reasons that biomass sorghum was observed to be more O<sub>3</sub>-tolerant than maize grown at the same field site (Yendrek, Eric, et al., 2017). However, sorghum genotypes were also found tolerant to O<sub>3</sub> in the growth chamber measurements where all leaves were exposed to similar O<sub>3</sub> concentrations. This indicates that other factors contribute significantly to defence against O<sub>3</sub> stress in sorghum.

It has been suggested that the detoxification capacity for O<sub>3</sub> in plants is associated with the capacity of photosynthetic CO<sub>2</sub> assimilation which provides energy for detoxification and repair and products for antioxidant biosynthesis (Massman, 2004; Musselman & Massman, 1999; Smirnov, 2000). In addition, the balance between A and g<sub>s</sub> was assumed as a key factor determining the extent of the O<sub>3</sub> response (Massman, 2004). Sorghum is less susceptible to drought than maize and has higher water-use-efficiency than other C<sub>4</sub> crops (Farré & Faci, 2006; Katerji & Mastrorilli, 2014; Steduto et al., 1997; Zegada-Lizarazu, Zatta, & Monti, 2012), indicating the potential for greater capacity for O<sub>3</sub> detoxification relative to stomatal O<sub>3</sub> uptake. However, other studies have shown that sorghum and maize have similar water-use-efficiency when water is non-limiting (Farré & Faci, 2006; Roby, Fernandez, Heaton, Miguez, & VanLoocke, 2017). Overall, intraspecific variation in O<sub>3</sub> tolerance is still unclear at a

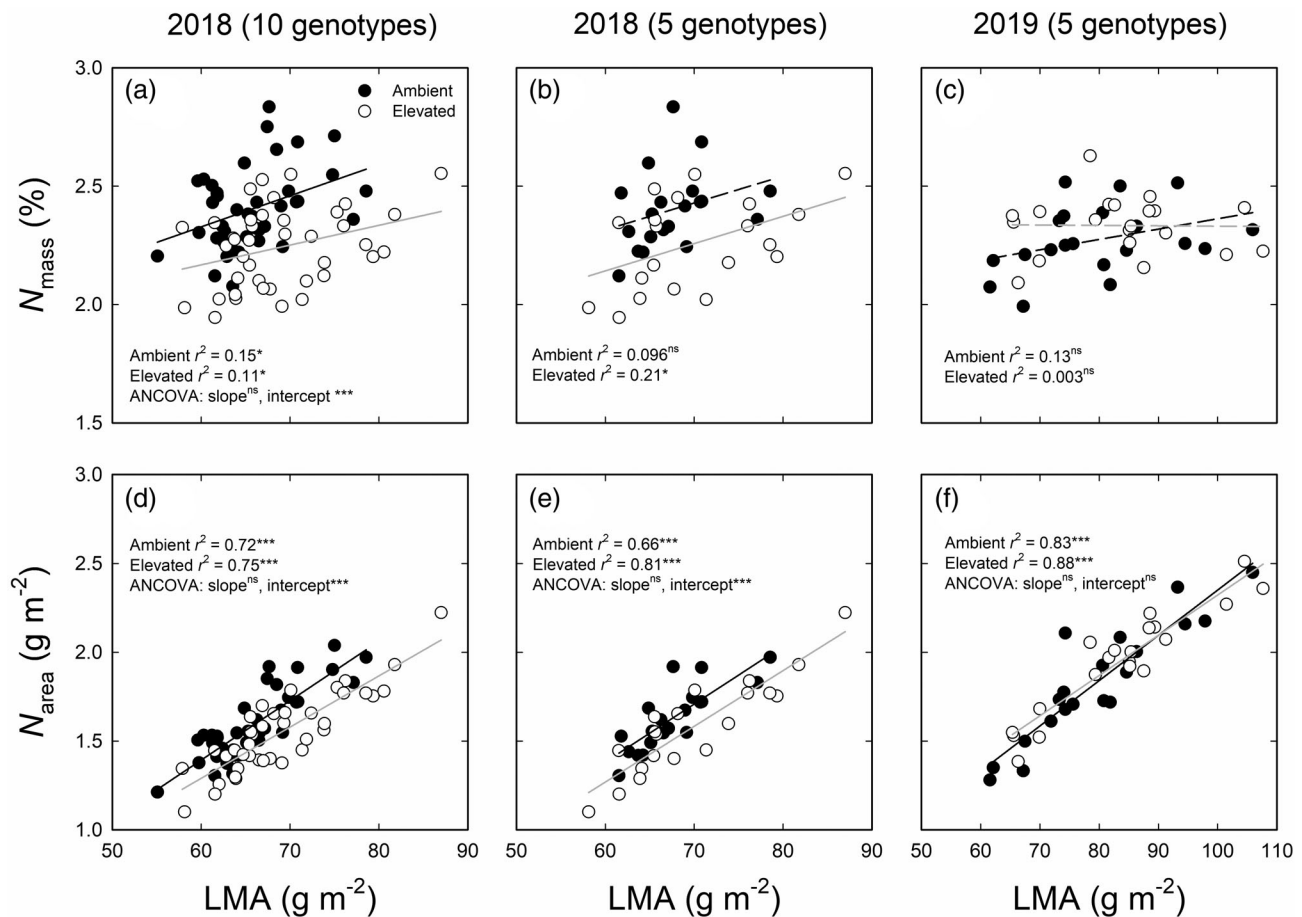


**FIGURE 8** The relationship between leaf dry mass per area (LMA) and leaf nitrogen content expressed on a mass basis (LMA and  $N_{\text{mass}}$ , a–c), and on an area basis (LMA and  $N_{\text{area}}$ , d–f) in 10 genotypes (a,d) and 5 genotypes (b,e) of sorghum grown under ambient and elevated  $\text{O}_3$  measured in 2018 and in 5 genotypes (c,f) of sorghum grown under ambient and elevated  $\text{O}_3$  measured in 2019. The data were fitted by linear regressions. Significant correlations are indicated by solid lines. ns, no significant difference ( $p > .05$ ); \* $p < .05$ ; \*\*\* $p < .001$

mechanistic level and will require future studies investigating plant response to  $\text{O}_3$  at both species and genotypic level.

### 4.3 | Implications for bioenergy feedstock breeding

Sorghum has emerged as a promising bioenergy feedstock. Sorghum is more water- and nitrogen-use efficient than corn and sugarcane, as well as being more drought tolerant and yielding more ethanol per unit area of land than many other biomass crops (Calviño & Messing, 2012; Regassa & Wortmann, 2014; Rooney et al., 2007). In addition, sorghum produces and stores fermentable sugar rather than starch in the stalks which can be metabolized by microbes to produce biofuels (Calviño & Messing, 2012; Regassa & Wortmann, 2014; Rooney et al., 2007). Previous studies have focused primarily on enhancement of sorghum biomass and sugar yield, conversion efficiency through genetic improvement, or agronomic management (Calviño & Messing, 2012; Carpita & McCann, 2008; Mullet et al., 2014; Regassa & Wortmann, 2014; Rooney et al., 2007). However, little effort has been

directed towards investigating yield stability, which is the most important factor for continuous ethanol production. Large yield and biomass losses to  $\text{O}_3$  pollution in maize and sugarcane may lead to a significant decrease in ethanol production with rising  $\text{O}_3$  concentrations in the future (Grantz & Vu, 2009; McGrath et al., 2015). Although switchgrass is tolerant to  $\text{O}_3$  and can be a candidate bioenergy feedstock, it produces a lower biomass than sorghum (Li et al., 2019; Rooney et al., 2007; Schmer et al., 2008; Wullschlegel et al., 2010). Our results provide evidence that sorghum genotypes exhibit greater  $\text{O}_3$  tolerance than other  $\text{C}_4$  bioenergy crops. Considering all the advantages of sorghum as a bioenergy crop, we suggest that sorghum can provide abundant and sustainable energy in the future.

## 5 | CONCLUSIONS

This first study demonstrates that there is a significant variability in plant functional traits across sorghum genotypes and that all genotypes showed a similar response to  $\text{O}_3$ . This study provides strong evidence that bioenergy sorghum genotypes are tolerant to  $\text{O}_3$  and maintain

high photosynthetic capacity in elevated O<sub>3</sub> concentrations. Furthermore, this study suggests that sorghum may have greater O<sub>3</sub> tolerance than other previously studied C<sub>4</sub> crops such as maize and switchgrass. These results have important implications for bioenergy feedstock development in response to climate changes. For instance, sorghum could be planted in regions with high O<sub>3</sub> pollution where O<sub>3</sub> concentrations cause a significant yield loss in other crops. Overall, the present results suggest that sorghum can produce high and stable biomass yields and provide sustainable energy under future climate scenarios.

## ACKNOWLEDGMENTS

We thank Jesse McGrath, Aidan McMahon, John Ferguson, Nicole Choquette, Anthony Digrado, Chris Montes, Duncan Martin, Hannah Demler, Renan Umburanas, Seldon Kwafo and Yanquan Zhang for technical and field assistance. We also thank Dr Samuel B. Fernandes and Dr John Ferguson for providing plant seeds and Prof. Andrew Leakey for helpful discussions. We thank two anonymous referees for their helpful comments. This work was funded by the DOE Center for Advanced Bioenergy and Bioproducts Innovation (U.S. Department of Energy, Office of Science, Office of Biological and Environmental Research under Award Number DE-SC0018420). Any opinions, findings, and conclusions or recommendations expressed in this publication are those of the author(s) and do not necessarily reflect the views of the U.S. Department of Energy or the U.S. Department of Agriculture (USDA). Mention of trade names or commercial products in this publication is solely for the purpose of providing specific information and does not imply recommendation or endorsement by the USDA. USDA is an equal opportunity provider and employer.

## CONFLICT OF INTEREST

The authors declare no conflicts of interest.

## AUTHOR CONTRIBUTIONS

Elizabeth A. Ainsworth and Shuai Li designed the study. Shuai Li, Christopher A. Moller and Noah G. Mitchell performed the measurements. Shuai Li performed the statistical analysis. Shuai Li, DoKyoung Lee and Elizabeth A. Ainsworth contributed to the interpretation of results. Shuai Li wrote the first version of the manuscript, which was reviewed and revised by all the authors.

## ORCID

Shuai Li  <https://orcid.org/0000-0003-2545-7763>

Elizabeth A. Ainsworth  <https://orcid.org/0000-0002-3199-8999>

## REFERENCES

- Ainsworth, E. A. (2017). Understanding and improving global crop response to ozone pollution. *Plant Journal*, *90*, 886–897.
- Ainsworth, E. A., & Long, S. P. (2005). What have we learned from 15 years of free-air CO<sub>2</sub> enrichment (FACE)? A meta-analytic review of the responses of photosynthesis, canopy properties and plant production to rising CO<sub>2</sub>. *New Phytologist*, *165*, 351–372.
- Ainsworth, E. A., Rogers, A., & Leakey, A. D. B. (2008). Targets for crop biotechnology in a future high-CO<sub>2</sub> and high-O<sub>3</sub> world. *Plant Physiology*, *147*, 13–19.
- Ainsworth, E. A., Rogers, A., Nelson, R., & Long, S. P. (2004). Testing the “source-sink” hypothesis of down-regulation of photosynthesis in elevated [CO<sub>2</sub>] in the field with single gene substitutions in *Glycine max*. *Agricultural and Forest Meteorology*, *122*, 85–94.
- Ainsworth, E. A., Yendrek, C. R., Sitch, S., Collins, W. J., & Emberson, L. D. (2012). The effects of tropospheric ozone on net primary productivity and implications for climate change. *Annual Review of Plant Biology*, *63*, 637–661.
- Atkinson, R. (2000). Atmospheric chemistry of VOCs and NO<sub>x</sub>. *Atmospheric Environment*, *34*, 2063–2101.
- Ball, J. T., Woodrow, I. E., & Berry, J. A. (1987). A model predicting stomatal conductance and its contribution to the control of photosynthesis under different environmental conditions. In J. Biggins (Ed.), *Progress in photosynthesis research* (pp. 221–224). Dordrecht, The Netherlands: Martinus Nijhoff.
- Bollero, G. A., Bullock, D. G., & Hollinger, S. E. (1996). Soil temperature and planting date effects on corn yield, leaf area, and plant development. *Agronomy Journal*, *88*, 385–390.
- Burkey, K. O., Booker, F. L., Ainsworth, E. A., & Nelson, R. L. (2012). Field assessment of a snap bean ozone bioindicator system under elevated ozone and carbon dioxide in a free air system. *Environmental Pollution*, *166*, 167–171.
- Calviño, M., & Messing, J. (2012). Sweet sorghum as a model system for bioenergy crops. *Current Opinion in Biotechnology*, *23*, 323–329.
- Carpita, N. C., & McCann, M. C. (2008). Maize and sorghum: Genetic resources for bioenergy grasses. *Trends in Plant Science*, *13*, 415–420.
- Chang, K.-L., Petropavlovskikh, I., Cooper, O. R., Schultz, M. G., & Wang, T. (2017). Regional trend analysis of surface ozone observations from monitoring networks in eastern North America, Europe and East Asia. *Elementa: Science of the Anthropocene*, *5*, 50.
- Choquette, N. E., Ainsworth, E. A., Bezodis, W., & Cavanagh, A. P. (2020). Ozone tolerant maize hybrids maintain Rubisco content and activity during long-term exposure in the field. *Plant Cell & Environment*, *43*, 3033–3047.
- Choquette, N. E., Ogut, F., Wertin, T. M., Montes, C. M., Sorgini, C. A., Morse, A. M., ... Ainsworth, E. A. (2019). Uncovering hidden genetic variation in photosynthesis of field-grown maize under ozone pollution. *Global Change Biology*, *25*, 4327–4338.
- Evans, J. R. (1989). Photosynthesis and nitrogen relationships in leaves of C<sub>3</sub> plants. *Oecologia*, *78*, 9–19.
- Farré, I., & Faci, J. M. (2006). Comparative response of maize (*Zea mays* L.) and sorghum (*Sorghum bicolor* L. Moench) to deficit irrigation in a Mediterranean environment. *Agricultural Water Management*, *83*, 135–143.
- Ferguson, J. N., Fernandes, S. B., Monier, B., Miller, N. D., Allan, D., Dmitrieva, A., ... Leakey, A. D. B. (2020). Machine learning enabled phenotyping for GWAS and TWAS of WUE traits in 869 field-grown sorghum accessions. *BioRxiv*. <https://doi.org/10.1101/2020.11.02.365213>.
- Fiscus, E. L., Booker, F. L., & Burkey, K. O. (2005). Crop responses to ozone: Uptake, modes of action, carbon assimilation and partitioning. *Plant Cell & Environment*, *28*, 997–1011.
- Flowers, M. D., Fiscus, E. L., Burkey, K. O., Booker, F. L., & Dubois, J.-J. B. (2007). Photosynthesis, chlorophyll fluorescence, and yield of snap bean (*Phaseolus vulgaris* L.) genotypes differing in sensitivity to ozone. *Environmental and Experimental Botany*, *61*, 190–198.
- Franks, P. J., Bonan, G. B., Berry, J. A., Lombardo, D. L., Holbrook, N. M., Herold, N., & Oleson, K. W. (2018). Comparing optimal and empirical stomatal conductance models for application in earth system models. *Global Change Biology*, *24*, 5708–5723.
- Frei, M., Tanaka, J. P., & Wissuwa, M. (2008). Genotypic variation in tolerance to elevated ozone in rice: Dissection of distinct genetic factors linked to tolerance mechanisms. *Journal of Experimental Botany*, *59*, 3741–3752.



- Gao, J., Zhu, B., Xiao, H., Kang, H., Hou, X., & Shao, P. (2015). A case study of surface ozone source apportionment during a high concentration episode, under frequent shifting wind conditions over the Yangtze River Delta, China. *Science of the Total Environment*, *544*, 853–863.
- Grantz, D. A., & Vu, H. B. (2009). O<sub>3</sub> sensitivity in a potential C<sub>4</sub> bioenergy crop: Sugarcane in California. *Crop Science*, *49*, 643–650.
- Grantz, D. A., Vu, H. B., Tew, T. L., & Veremis, J. C. (2012). Sensitivity of gas exchange parameters to ozone in diverse C<sub>4</sub> sugarcane hybrids. *Crop Science*, *52*, 1270–1280.
- Guidi, L., Degl'Innocenti, E., Martinelli, F., & Piras, M. (2009). Ozone effects on carbon metabolism in sensitive and insensitive *Phaseolus* cultivars. *Environmental and Experimental Botany*, *66*, 117–125.
- Hoshika, Y., Osada, Y., de Marco, A., Peñuelas, J., & Paoletti, E. (2018). Global diurnal and nocturnal parameters of stomatal conductance in woody plants and major crops. *Global Ecology and Biogeography*, *27*, 257–275.
- Katerji, N., & Mastrorilli, M. (2014). *Water use efficiency of cultivated crops*. Chichester, England: John Wiley & Sons.
- Lawrence, C. J., & Walbot, V. (2007). Translational genomics for bioenergy production from fuelstock grasses: Maize as the model species. *The Plant Cell*, *19*, 2091–2094.
- Leakey, A. D. B., Bernacchi, C. J., Ort, D. R., & Long, S. P. (2006). Long-term growth of soybean at elevated [CO<sub>2</sub>] does not cause acclimation of stomatal conductance under fully open-air conditions. *Plant, Cell & Environment*, *29*, 1794–1800.
- Leakey, A. D. B., Ferguson, J. N., Pignon, C. P., Wu, A., Jin, Z., Hammer, G. L., & Lobell, D. B. (2019). Water use efficiency as a constraint and target for improving the resilience and productivity of C<sub>3</sub> and C<sub>4</sub> crops. *Annual Review of Plant Biology*, *70*, 781–808.
- Leakey, A. D. B., Urbelarra, M., Ainsworth, E. A., Naidu, S. L., Rogers, A., Ort, D. R., & Long, S. P. (2006). Photosynthesis, productivity, and yield of maize are not affected by open-air elevation of CO<sub>2</sub> concentration in the absence of drought. *Plant Physiology*, *140*, 779–790.
- Leitao, L., Bethenod, O., & Biolley, J.-P. (2007). The impact of ozone on juvenile maize (*Zea mays* L.) plant photosynthesis: Effect on vegetative biomass, pigmentation, and carboxylases (PEPc and rubisco). *Plant Biology*, *9*, 478–488.
- Leitao, L., Maoret, J.-J., & Biolley, J.-P. (2007). Changes in PEP carboxylase, rubisco and rubisco activase mRNA levels from maize (*Zea mays*) exposed to a chronic ozone stress. *Biological Research*, *40*, 137–153.
- Li, S., Courbet, G., Ourry, A., & Ainsworth, E. A. (2019). Elevated ozone concentration reduces photosynthetic carbon gain but does not alter leaf structural traits, nutrient composition or biomass in switchgrass. *Plants*, *8*, 85.
- Li, S., Harley, P. C., & Niinemets, Ü. (2017). Ozone-induced foliar damage and release of stress volatiles is highly dependent on stomatal openness and priming by low-level ozone exposure in *Phaseolus vulgaris*. *Plant, Cell & Environment*, *40*, 1984–2003.
- Li, S., Tosens, T., Harley, P. C., Jiang, Y., Kanagendran, A., Grosberg, M., ... Niinemets, Ü. (2018). Glandular trichomes as a barrier against atmospheric oxidative stress: Relationships with ozone uptake, leaf damage, and emission of LOX products across a diverse set of species. *Plant, Cell & Environment*, *41*, 1263–1277.
- Li, S., Zhang, Y.-J., Sack, L., Scoffoni, C., Ishida, A., Chen, Y.-J., & Cao, K.-F. (2013). The heterogeneity and spatial patterning of structure and physiology across the leaf surface in giant leaves of *Alocasia macrorrhiza*. *PLoS One*, *8*, e66016.
- Lin, Y.-S., Medlyn, B. E., Duursma, R. A., Prentice, I. C., Wang, H., Baig, S., ... Wingate, L. (2015). Optimal stomatal behaviour around the world. *Nature Climate Change*, *5*, 459–464.
- Lombardozzi, D., Sparks, J. P., Bonan, G., & Levis, S. (2012). Ozone exposure causes a decoupling of conductance and photosynthesis: Implications for the Ball–Berry stomatal conductance model. *Oecologia*, *169*, 651–659.
- Long, S. P., Ainsworth, E. A., Rogers, A., & Ort, D. R. (2004). Rising atmospheric carbon dioxide: Plants FACE the future. *Annual Review of Plant Biology*, *55*, 591–628.
- Long, S. P., & Bernacchi, C. J. (2003). Gas exchange measurements, what can they tell us about the underlying limitations to photosynthesis? Procedures and sources of error. *Journal of Experimental Botany*, *54*, 2393–2401.
- Long, S. P., & Naidu, S. L. (2002). Effects of oxidants at the biochemical, cell and physiological levels. In J. M. B. Bell & M. J. Treshow (Eds.), *Air pollution and plants* (pp. 69–88). London, England: Wiley.
- Markelz, R. J. C., Strellner, R. S., & Leakey, A. D. B. (2011). Impairment of C<sub>4</sub> photosynthesis by drought is exacerbated by limiting nitrogen and ameliorated by elevated [CO<sub>2</sub>] in maize. *Journal of Experimental Botany*, *62*, 3235–3246.
- Massman, W. J. (2004). Toward an ozone standard to protect vegetation based on effective dose: A review of deposition resistances and a possible metric. *Atmospheric Environment*, *38*, 2323–2337.
- Masutomi, Y., Kinose, Y., Takimoto, T., Yonekura, T., Oue, H., & Kobayashi, K. (2019). Ozone changes the linear relationship between photosynthesis and stomatal conductance and decreases water use efficiency in rice. *Science of the Total Environment*, *655*, 1009–1016.
- Maughan, M., Voigt, T., Parrish, A., Bollero, G., Rooney, W., & Lee, D. K. (2012). Forage and energy sorghum responses to nitrogen fertilization in central and southern Illinois. *Agronomy Journal*, *104*, 1032–1040.
- McGrath, J. M., Betzelberger, A. M., Wang, S., Shook, E., Zhu, X.-G., Long, S. P., & Ainsworth, E. A. (2015). An analysis of ozone damage to historical maize and soybean yields in the United States. *Proceedings of the National Academy of Sciences of the United States of America*, *112*, 14390–14295.
- Medlyn, B. E., Duursma, R. A., Eamus, D., Ellsworth, D. S., Prentice, I. C., Barton, C. V. M., ... Wingate, L. (2011). Reconciling the optimal and empirical approaches to modelling stomatal conductance. *Global Change Biology*, *17*, 2134–2144.
- Mills, G., Sharps, K., Simpson, D., Pleijel, H., Broberg, M., Uddling, J., ... Dingenen, R. V. (2018a). Ozone pollution will compromise efforts to increase global wheat production. *Global Change Biology*, *24*, 3560–3574.
- Mills, G., Sharps, K., Simpson, D., Pleijel, H., Frei, M., Burkey, K., ... Agrawal, M. (2018b). Closing the global ozone yield gap: Quantification and cobenefits for multistress tolerance. *Global Change Biology*, *24*, 4869–4893.
- Miner, G. L., & Bauerle, W. L. (2017). Seasonal variability of the parameters of the Ball–Berry model of stomatal conductance in maize (*Zea mays* L.) and sunflower (*Helianthus annuus* L.) under well-watered and water-stresses conditions. *Plant, Cell & Environment*, *40*, 1874–1886.
- Monks, P. S., Archibald, A. T., Colette, A., Cooper, O., Coyle, M., Derwent, R., ... Williams, M. L. (2015). Tropospheric ozone and its precursors from the urban to the global scale from air quality to short-lived climate forcer. *Atmospheric Chemistry and Physics*, *15*, 8889–8973.
- Morgan, P. B., Bernacchi, C. J., Ort, D. R., & Long, S. P. (2004). An *in vivo* analysis of the effect of season-long open-air elevation of ozone to anticipated 2050 levels on photosynthesis in soybean. *Plant Physiology*, *135*, 2348–2357.
- Morgan, P. B., Mies, T. A., Bollero, G. A., Nelson, R. L., & Long, S. P. (2006). Season-long elevation of ozone concentration to projected 2050 levels under fully open-air conditions substantially decreases the growth and production of soybean. *New Phytologist*, *170*, 333–343.
- Moura, B. B., Hoshika, Y., Ribeiro, R. V., & Paoletti, E. (2018). Exposure- and flux-based assessment of ozone risk to sugarcane plants. *Atmospheric Environment*, *176*, 252–260.
- Mullet, J., Morishige, D., McCormick, R., Truong, S., Hilley, J., McKinley, B., ... Rooney, W. (2014). Energy sorghum – A genetic model for the design of C<sub>4</sub> grass bioenergy crops. *Journal of Experimental Botany*, *65*, 3479–3489.

- Musselman, R. C., & Massman, W. J. (1999). Ozone flux to vegetation and its relationship to plant response and ambient air quality standards. *Atmospheric Environment*, 33, 65–73.
- Oikawa, S., & Ainsworth, E. A. (2016). Changes in leaf area, nitrogen content and canopy photosynthesis in soybean exposed to an ozone concentration gradient. *Environmental Pollution*, 215, 347–355.
- Oksanen, E., Riikonen, J., Kaakinen, S., Holopainen, T., & Vapaacuori, E. (2005). Structural characteristics and chemical composition of birch (*Betula pendula*) leaves are modified by increasing CO<sub>2</sub> and ozone. *Global Change Biology*, 11, 732–748.
- Paoletti, E., & Grulke, N. E. (2010). Ozone exposure and stomatal sluggishness in different plant physiognomic classes. *Environmental Pollution*, 158, 2664–2671.
- Regassa, T. H., & Wortmann, C. S. (2014). Sweet sorghum as a bioenergy crop: Literature review. *Biomass and Bioenergy*, 64, 348–355.
- Reid, W. V., Ali, M. K., & Field, C. B. (2020). The future for bioenergy. *Global Change Biology*, 26, 264–286.
- Roby, M. C., Fernandez, M. G. S., Heaton, E. A., Miguez, F. E., & VanLoocke, A. (2017). Biomass sorghum and maize have similar water-use-efficiency under non-drought conditions in the rain-fed Midwest U.S. *Agricultural and Forest Meteorology*, 247, 434–444.
- Rooney, W. L., & Aydin, S. (1999). Genetic control of a photoperiod-sensitive response in *Sorghum bicolor* (L.) Moench. *Crop Science*, 39, 397–400.
- Rooney, W. L., Blumenthal, J., Bean, B., & Mullet, J. E. (2007). Designing sorghum as a dedicated bioenergy feedstock. *Biofuels Bioproducts & Biorefining*, 1, 147–157.
- Schmer, M. R., Vogel, K. P., Mitchell, R. B., & Perrin, R. K. (2008). Net energy of cellulosic ethanol from switchgrass. *Proceedings of the National Academy of Sciences of the United States of America*, 105, 464–469.
- Singh, A. A., Agrawal, S. B., Shahi, J. P., & Agrawal, M. (2014). Assessment of growth and yield losses in two *Zea mays* L. cultivars (quality protein maize and nonquality protein maize) under projected levels of ozone. *Environmental Science and Pollution Research*, 21, 2628–2641.
- Smirnoff, N. (2000). Ascorbic acid: Metabolism and functions of a multifaceted molecule. *Current Opinion in Plant Biology*, 3, 229–235.
- Steduto, P., Katerji, N., Puertos-Molina, H., Ünü, M., Mastroilli, M., & Rana, G. (1997). Water-use efficiency of sweet sorghum under water stress conditions gas-exchange investigations at leaf and canopy scales. *Field Crops Research*, 54, 221–234.
- Tilman, D., Socolow, R., Foley, J. A., Hill, J., Larson, E., Lynd, L., ... Williams, R. (2009). Beneficial biofuels—the food, energy, and environment trilemma. *Science*, 325, 270–271.
- Valluru, R., Gazave, E. E., Fernandes, S. B., Ferguson, J. N., Lozano, R., Hirannaiah, P., ... Bandillo, N. (2019). Deleterious mutation burden and its association with complex traits in sorghum (*Sorghum bicolor*). *Genetics*, 211, 1075–1087.
- Verma, N., Lakhani, A., & Kumari, K. M. (2017). High ozone episodes at a semi-urban site in India: Photochemical generation and transport. *Atmospheric Research*, 197, 232–243.
- von Caemmerer, S. (2000). *Biochemical models of leaf photosynthesis*. Collingwood, Australia: CSIRO.
- Wilkinson, S., Mills, G., Illidge, R., & Davies, W. J. (2012). How is ozone pollution reducing our food supply? *Journal of Experimental Botany*, 63, 527–536.
- Wittig, V. E., Ainsworth, E. A., Naidu, S. L., Karnosky, D. F., & Long, S. P. (2009). Quantifying the impact of current and future tropospheric ozone on tree biomass, growth, physiology and biochemistry: A quantitative meta-analysis. *Global Change Biology*, 15, 396–424.
- Wolz, K. J., Wertin, T. M., Abordo, M., Wang, D., & Leakey, A. D. B. (2017). Diversity in stomatal function is integral to modelling plant carbon and water flux. *Nature Ecology & Evolution*, 1, 1292–1298.
- Wullschlegel, S. D., Davis, E. B., Borsuk, M. E., Gunderson, C. A., & Lynd, L. R. (2010). Biomass production in switchgrass across the United States: Database description and determinants of yield. *Agronomy Journal*, 102, 1158–1168.
- Yendrek, C. R., Erice, G., Montes, C. M., Tomaz, T., Sorgini, C. A., Brown, P. J., ... Ainsworth, E. A. (2017). Elevated ozone reduces photosynthetic carbon gain by accelerating leaf senescence of inbred and hybrid maize in a genotype-specific manner. *Plant, Cell & Environment*, 40, 3088–3100.
- Yendrek, C. R., Leisner, C. P., & Ainsworth, E. A. (2013). Chronic ozone exacerbates the reduction in photosynthesis and acceleration of senescence caused by limited N availability in *Nicotiana sylvestris*. *Global Change Biology*, 19, 3155–3166.
- Yendrek, C. R., Tomaz, T., Montes, C. M., Cao, Y., Morse, A. M., Brown, P. J., ... Ainsworth, E. A. (2017). High-throughput phenotyping of maize leaf physiological and biochemical traits using hyperspectral reflectance. *Plant Physiology*, 173, 614–626.
- Young, P. J., Archibald, A. T., Bowman, K. W., Lamarque, J.-F., Naik, V., Stevenson, D. S., ... Zeng, G. (2013). Pre-industrial to end 21st century projections of tropospheric ozone from the atmospheric chemistry and climate model intercomparison project (ACC-MIP). *Atmospheric Chemistry and Physics*, 13, 2063–2090.
- Yuan, J. S., Tiller, K. H., Al-Ahman, H., Stewart, N. R., & Stewart, C. N., Jr. (2008). Plants to power: Bioenergy to fuel the future. *Trends in Plant Science*, 13, 421–429.
- Zegada-Lizarazu, W., Zatta, A., & Monti, A. (2012). Water uptake efficiency and above- and belowground biomass development of sweet sorghum and maize under different water regimes. *Plant and Soil*, 351, 47–60.
- Zhang, L., Xiao, S., Chen, Y. J., Xu, H., Li, Y. G., Zhang, Y. W., & Luan, F. S. (2017). Ozone sensitivity of four Pakchoi cultivars with different leaf colors: Physiological and biochemical mechanisms. *Photosynthetica*, 55, 478–490.
- Zhen, S., & Bugbee, B. (2020). Steady-state stomatal responses of C<sub>3</sub> and C<sub>4</sub> species to blue light fraction: Interactions with CO<sub>2</sub> concentration. *Plant Cell & Environment*, 43, 3020–3032. <https://doi.org/10.1111/pce.13888>

## SUPPORTING INFORMATION

Additional supporting information may be found online in the Supporting Information section at the end of this article.

**How to cite this article:** Li S, Moller CA, Mitchell NG, Lee DK, Ainsworth EA. Bioenergy sorghum maintains photosynthetic capacity in elevated ozone concentrations. *Plant Cell Environ*. 2021;44:729–746. <https://doi.org/10.1111/pce.13962>